

This article was downloaded by: [Tomsk State University of Control Systems and Radio]

On: 19 February 2013, At: 14:18

Publisher: Taylor & Francis

Informa Ltd Registered in England and Wales Registered Number: 1072954

Registered office: Mortimer House, 37-41 Mortimer Street, London W1T 3JH, UK



Molecular Crystals and Liquid Crystals

Publication details, including instructions for authors and subscription information:

<http://www.tandfonline.com/loi/gmcl16>

The Effect of Molecular Structure on the Formation of Induced Nematic Phases in Binary Mixtures

Mary E. Neubert^a, Katherine Leung^{a b} & Welf A. Saupe^a

^a Liquid Crystal Institute, Kent State University, Kent, Ohio, 44242

^b Uniroyal, Mishawaka, IN.

Version of record first published: 28 Mar 2007.

To cite this article: Mary E. Neubert, Katherine Leung & Welf A. Saupe (1986): The Effect of Molecular Structure on the Formation of Induced Nematic Phases in Binary Mixtures, *Molecular Crystals and Liquid Crystals*, 135:3-4, 283-342

To link to this article: <http://dx.doi.org/10.1080/00268948608084815>

PLEASE SCROLL DOWN FOR ARTICLE

Full terms and conditions of use: <http://www.tandfonline.com/page/terms-and-conditions>

This article may be used for research, teaching, and private study purposes. Any substantial or systematic reproduction, redistribution, reselling, loan, sub-licensing, systematic supply, or distribution in any form to anyone is expressly forbidden.

The publisher does not give any warranty express or implied or make any representation that the contents will be complete or accurate or up to

date. The accuracy of any instructions, formulae, and drug doses should be independently verified with primary sources. The publisher shall not be liable for any loss, actions, claims, proceedings, demand, or costs or damages whatsoever or howsoever caused arising directly or indirectly in connection with or arising out of the use of this material.

The Effect of Molecular Structure on the Formation of Induced Nematic Phases in Binary Mixtures

MARY E. NEUBERT, KATHERINE LEUNG,[†] and WELF A. SAUPE

Liquid Crystal Institute, Kent State University, Kent, Ohio 44242

(Received June 18, 1985)

A variety of 4-halophenyl-4'-alkoxybenzoates and 4-alkoxyphenyl-4'-halobenzoates were synthesized, their mesomorphic properties determined and compared with those of the analogous halo anils. The ability of these esters to form induced nematic phases (INPs) in binary mixtures was studied along with a variety of other mesogenic type compounds not having a nematic phase. The contact method was used to screen 258 mixtures for INPs in an attempt to determine which molecular structural features favored formation of this phase in binary mixtures. INPs were observed in many of these mixtures and with a wide variety of structures. Phase diagrams of some of these mixtures were obtained in order to compare the abilities of certain structural features to form INPs. Two types of diagrams were observed. Type I showed a narrow INP range occurring over most of the composition range between two nearly linear SN and MI curves and was observed only when the two components had similar molecular lengths either short or long. In Type II, wide range INPs were observed between a nearly linear MI curve and a non-linear SN curve with their maximum range in the region of the minimum and was observed only when the two components had a large difference between their molecular lengths. The range of these INPs was largest at compositions of <50% of the longest molecule. Phase diagrams also indicated that the INP was less favored as either the alkyl chain length or the halogen size increased. The steric effect of an α -methyl group on the acid alkyl chain in the 4-alkoxyphenyl-4'-alkylbenzoates on nematic properties reported earlier was also observed with INPs in these mixtures.

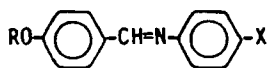
Keywords: liquid crystals, mixtures, induced nematic phases, esters, anils

INTRODUCTION

Earlier reports in the literature that alkoxy anils containing a terminal halogen atom 1 exhibited smectic B (S_B) phases¹⁻⁷ had prompted us

[†] Present address: Uniroyal, Mishawaka, IN.

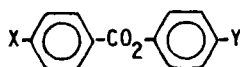
to prepare a number of phenylbenzoates containing terminal halogen



where $X = F, Cl, Br, I$

1

atoms **2** and **3** to determine if the smectic B phases would also be



2a $X = R, Y = F \text{ or } I$

b $X = RO, Y = F, Cl, Br \text{ or } I$

3 $X = F \text{ or } I, Y = RO$

observed in these compounds. We prepared those chain lengths which past experience had taught us would most likely have smectic phases i.e. mid-chain lengths C_4 — C_8 and C_{10} . Transition temperatures for these esters are presented in Table I. When the halogen was located on the acid end **3**, no mesophases were observed when $Y = RO$. The analogs with $Y = R$ therefore were not prepared since these would be expected to be even less likely to show mesophases. When the halogen was moved to the phenolic end **2**, smectic A (S_A) phases were observed when $X = RO$ but no mesophases when $X = R$. The S_A phase did not begin to appear until $R = C_6$ but persisted even into the C_{14} homolog and occurred with all the halogens even with the bulky iodide. No S_B phases were observed in any of these esters.

A plot of the transition temperatures for the halo esters **2b** for $R = C_{10}H_{21}$ versus halogen (Figure 1) shows that all the transition temperatures rise with increasing halogen size. However, the phase range of the S_A phase first increases from being monotropic at $Y = F$ reaching a maximum at $Y = Cl$ and then decreases. The same plot for the halo anils with $R = C_8H_{17}$ (Figure 2) shows similar trends. Unlike the esters, these compounds have a wide-range S_B phase in addition to the S_A . Most of the melting points for the anils are lower than those for the esters but the clearing temperatures are higher giving a wider range over which mesophases occur. The S_A phase ranges for $Y = Cl$ and Br are approximately the same in both series but when $Y = I$, the S_A phase disappears in the anils but persists in

TABLE I
Transition temperatures (°C) for halo esters

X	Y	C ¹	S _A	N	I
F	OC ₆ H ₁₃	59.4		--	64.9-65.8
F	OC ₁₀ H ₂₁	78.7		--	75.5-83.4
F	OC ₁₄ H ₂₉	74.4		--	89.8-91.5
I	OC ₆ H ₁₃	107.2		--	111.1-113.5
I	OC ₁₀ H ₂₁	113.3-115.4		--	112.4-116.3
I	OC ₁₄ H ₂₉	114.4		--	115.2-118.2
C ₄ H ₉	F	9.5		--	34.5-35.1
C ₆ H ₁₃	I	51.9		--	65.9-67.2
C ₁₀ H ₂₁	I	84.2		--	101.9-102.8
C ₄ H ₉	F	73.6		--	97.5-98.7
C ₆ H ₁₃ ⁰	F	37.5	(37.5-38.3) ²	--	59.5-60.4
C ₈ H ₁₇ ⁰	F	43.6	(43.3-43.8)	--	58.7-59.2
C ₁₀ H ₂₁ ⁰	F	41.6	(46.3)	--	64.6-65.0
H	Cl	53.9	--	--	60.8-61.5
C ₄ H ₉	Cl	93.3	--	--	104.0-104.9 ³
C ₆ H ₁₃ ⁰	Cl	70.7	--	--	82.5-85.8
C ₈ H ₁₇ ⁰	Cl	58.0	75.4-75.7		78.2-79.3
C ₁₀ H ₂₁ ⁰	Cl	49.9	70.4	--	78.1-78.7 ³
C ₄ H ₉ ⁰	Br	107.4	--	--	116.9-117.6
C ₁₀ H ₂₁ ⁰	Br	61	79.8	--	85.1
C ₆ H ₁₃ ⁰	I	84.2	--	--	101.9-102.8
C ₁₀ H ₂₁ ⁰	I	67.9	85.5-86.2	--	86.8-87.0
C ₁₂ H ₂₅ ⁰	I	66.0	78.2	--	86.0-86.8
C ₁₄ H ₂₉ ⁰	I	65.6	(84.1-84.9)	--	85.4-86.5

¹ Crystallization temperature observed at a cooling rate of 2°/min.

² () indicates a monotropic transition.

³ Previously reported in Ref. 1.

the esters although at a much shorter range. In both series, the S_A phase is monotropic when Y = F. Some care must be taken in making such detailed comparisons in that R is not the same in both series.

It is not surprising to find an increase in transition temperatures with increasing halogen size since the molecular weights also increase. Molecular models (Ealing CPIC) show that even the bulky iodide

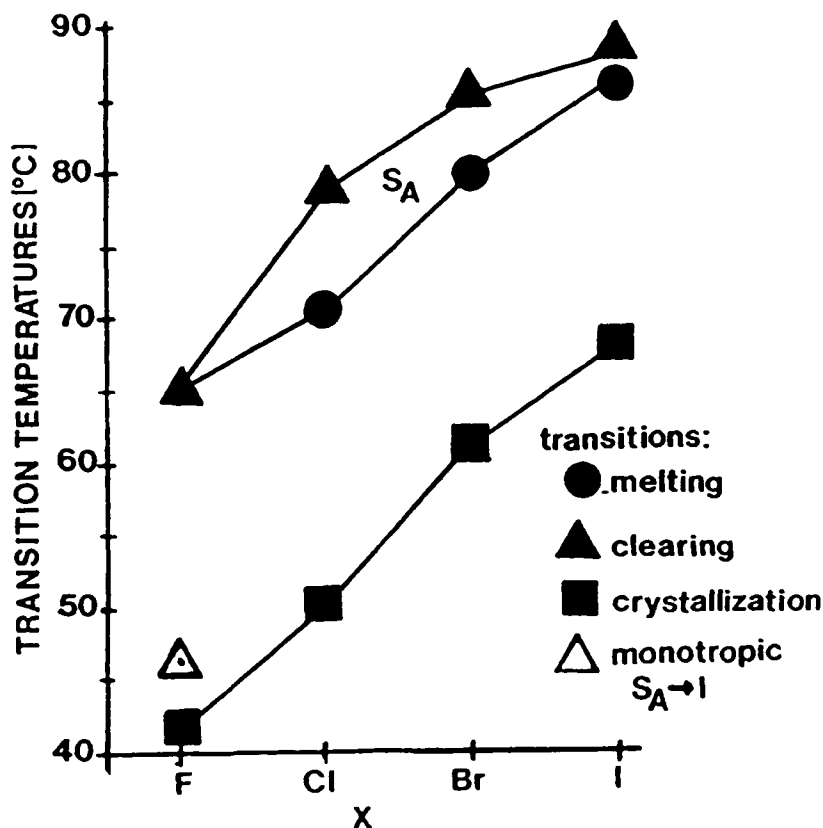
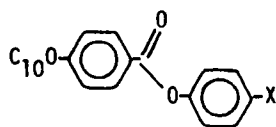
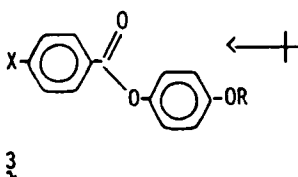
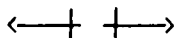
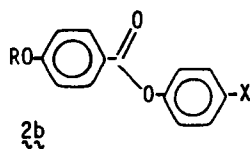
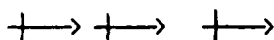


FIGURE 1 Transition temperatures ($^{\circ}\text{C}$) versus halogen (X) for



atom fits into the molecular diameter of these molecules. The lower coplanarity of the central ester group as compared to the anil allows for a larger volume for the iodide atom in the ester molecule and this provides a possible explanation for the loss of the S_A phase in the anil when $Y = I$ but not in the ester. The greater tendency for the **2b** esters to form S_A phases over the **3** series has been explained by Malthete's group as due to an alignment of the dipoles in one direction in series **2b** as compared to the opposing terminal dipoles to the central dipole for series **3** in either the esters or the anils.¹



X-ray studies on the anils have suggested a model in which the halogen ends alternate as shown in Figure 3.⁸ This would require a bilayer structure with some folding of the chains. De Vries, however, feels that the x-ray patterns for the S_A phase in the halo anils can be explained by a single layer S_A phase.⁹ More detailed x-ray studies are needed to resolve this problem.

Although these results were interesting, the poor mesomorphism of these halo phenylbenzoates caused us to discontinue any further studies of these esters at this time. However, the recent observance of an induced nematic phase (INP) in binary mixtures of 2-fluorenylethylidene-4'-*n*-dodecylaniline (FC12A) and 4-*n*-butoxybenzylidene-4'-chloroaniline (40.Cl) both of which exhibit only S_A phases⁹ convinced us that we should investigate similar mixtures containing halo esters. Such INPs could be useful in the design of materials for nematic displays and there also was the possibility that induced smectic phases would be observed in similar mixtures. No attempt was made in the report on INPs in mixtures of FC12A and 40.Cl to determine which molecular features of these two components were needed to observe INPs. We were interested in determining these structural features to be used as an aid in designing mixtures which would form INPs as well as determining if the halo esters would also form INPs in binary mixtures.

MIXTURE STUDIES

INPs are not new having been reported in early mixture studies,^{10,11} by Demus and Sackmann in their smectic identification work¹²⁻¹⁴ and

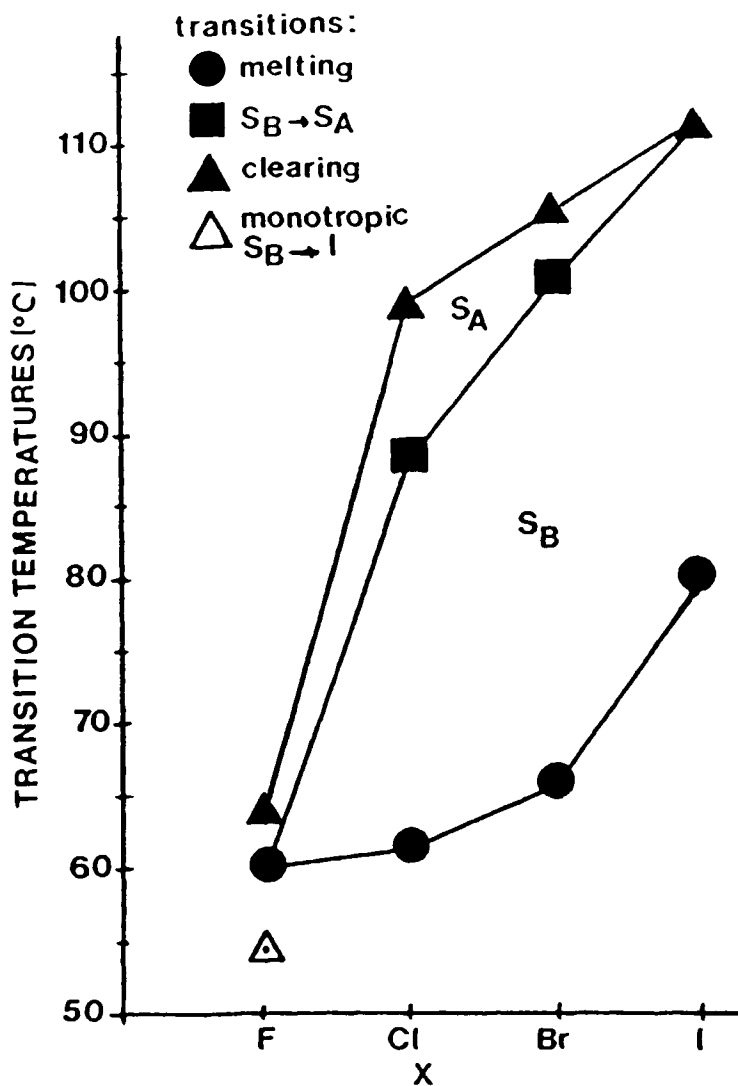
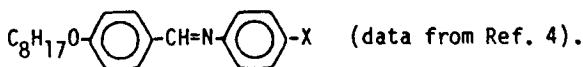


FIGURE 2 Transition temperatures (°C) versus halogen (X) for



in more recent mixture studies.¹⁵⁻¹⁸ None of this research was designed to study INPs or the relationship between their formation and the molecular structures of their components.

Our investigation began by studying three structural features: the

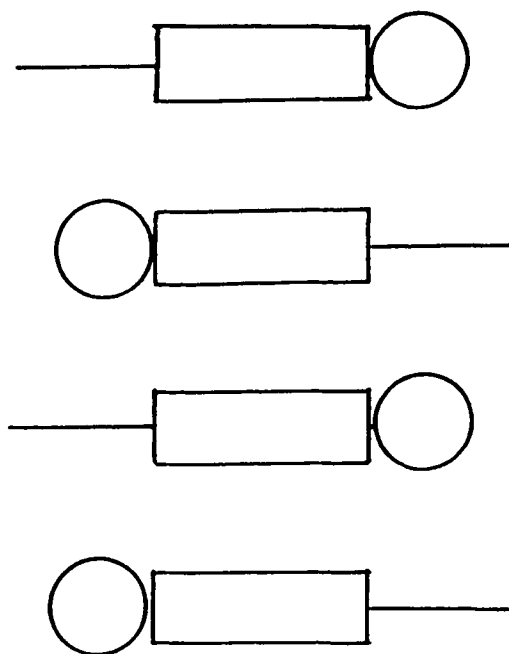


FIGURE 3 Alternating packing of molecules in the S_A phase of the halo anils

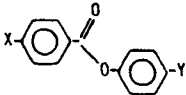
halogen atom, the fluorene ring system and the central anil group and expanded rapidly to other structural features as well. Even with the initial limited molecular modifications, it was obvious that attempting to do phase diagrams of the necessary mixtures to determine if INPs were formed would be too time consuming. Thus, we chose to use the well known contact method^{19†} for screening the mixtures for INPs and phase diagrams for comparing INP ranges.

The similar biphenyl anil **4a** was first tried as a replacement for the fluorene anil **4b** in mixtures with a variety of halo anils as shown in Table VII.‡ INPs were observed in all the biphenyl mixtures (Nos. 3, 5, 9, 11) that were observed in the fluorene mixtures (Nos. 4, 6, 10, and 12) except in mixture 1 indicating that the fluorene ring is not necessary to observe INPs. These mixture studies also showed

† Although this method is widely used, a detailed description can only be found in the German literature. Consequently, we have described the procedure we used in the experimental section in order to aid those new to this area.

‡ Transition temperature data for all the components used in the mixtures studied are given in Tables I–VI.

TABLE II
Transition temperatures (°C) for

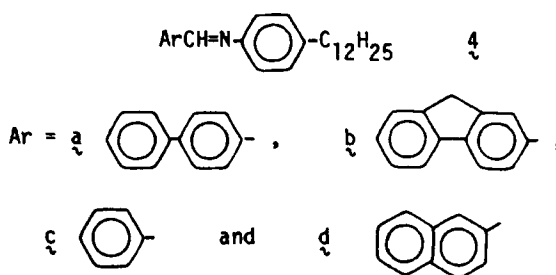


X	Y	C ¹	S _A	N	I
H	H	40			67.2-78.3
C ₄ H ₉ O	H	81.9			90.4-91.5
H	OC ₄ H ₉	36.8			67.5-68.2
C ₆ H ₁₃	OCH ₃	31.1			63.2-65.2
Me ₂ CH	OCH ₃	67.6			96.4-98.0 ²
EtCH(Me)-	OCH ₃	51.4			81.7-85.0 ²
EtCH(Me)-	OC ₃ H ₇	51.1			79.5-82.7 ²
EtCH(Me)-	OC ₆ H ₁₃	17.9			44.9-46.8 ²
EtCH(Me)-	OC ₈ H ₁₇	17.5			33.0-34.3 ²
Me ₂ CHCH ₂	OCH ₃	47.4			67.6-69.0 ²
Me ₂ CHCH ₂	OC ₂ H ₅	49.0			78.9-79.7 ²
Me ₂ CHCH ₂	OC ₃ H ₇	28.1			65.2-67.5 ²
C ₉ H ₁₉ O	NO ₂	49.2			56.7-59.0
C ₁₀ H ₂₁ O	NO ₂	34	51.8-53.6	- -	76.5-76.9 ³

¹ Crystallization temperature observed at a cooling rate of 2°/min.

² Data from Ref. 22.




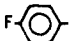
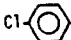
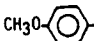
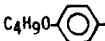
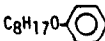


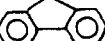

³ Previously reported by A. C. Griffin, R. F. Fisher, and S. J. Havens, *J. Am. Chem. Soc.* **100**, 6329 (1978).



that an alkoxy group was not needed on the aldehyde end of the anil (Nos. 2 and 9-12) but if this alkoxy chain was too long no INPs were observed (Nos. 7 and 8). It did not seem to matter whether the chlorine atom was on the aniline (Nos. 3 and 4) or the aldehyde end (Nos. 11 and 12).

Both the biphenyl **4a** and the fluorene **4b** anils were used in mixtures

TABLE III
Transition temperatures (°C) for

$\text{ArCH=N}-\text{C}_6\text{H}_4-\text{Y}$						
Ar	Y	C^1	S_E	S_B	S_A	I
	C ₁₂ H ₂₅	34.4				47.8-48.0
	Cl	51.9				60.8-61.5
	C ₁₂ H ₂₅	53.3				58.6-59.2
	Cl	51.6				70.0-72.3
	OCH ₃	99.2 (C ₁)				121.9-123.7
	Cl	76.5				92.1-92.6 ⁴
	Cl	72.9		84.4-84.6 ⁷	89.5-89.8	90.3-90.6 ⁴
	Cl	50		67.2-67.9 ⁷	89.0-89.2	99.8-100.0 ⁴
	C ₂ H ₅	116.7				122.0-122.4 ⁵
	C ₁₂ H ₂₅	84.2	- ⁶	100.6-101.0 ⁷	119	125.9-126.1 ⁵
	C ₁₂ H ₂₅	82.7			117.5-118.0	141.6 ⁸
	C ₁₂ H ₂₅	61.6 ⁹				65.1-67.2

¹ Crystallization temperature at a cooling rate of 2°/min.

² Crystallization occurred at 99.2° but these crystals quickly converted to another form at 99.1°. On reheating the reverse transition occurred at 114.0–115.0.

³ Previously reported in Ref. 1.

⁴ Previously reported in Ref. 6.

⁵ Previously reported in Ref. 2.

⁶ Goodby reported observing a S_E phase at 83.8°. Our material began to crystallize at 84.2 but by moving the slide we were able to find an area still in the S_B phase and cool to 82.3. Still we could not see the S_E phase. J. W. Goodby, *Liquid Crystals and Ordered Fluids*, Vol. 4, ed. A. C. Griffin and J. F. Johnson (Plenum Press, 1984), p. 175.

⁷ Transition bars were observed in the S_B ↔ S_A transitions.

⁸ Previously reported in Ref. 9.

⁹ Also cooled rapidly to give a crystallization temperature of 56.8° without observing a nematic phase.

TABLE IV
Transition temperatures (°C) for

$\text{RO}-\text{C}_6\text{H}_4-\text{C}_6\text{H}_4-\text{CO}_2\text{R}'$						
<u>R</u>	<u>R'</u>	<u>C</u> ¹	<u>S_E</u>	<u>S_B</u>	<u>S_A</u>	<u>I</u>
CH ₃	C ₄ H ₉	54				76.5- 78.0
CH ₃	C ₆ H ₁₃	44.8	(44.9- 45.4) ²			59.0- 61.7
CH ₃	C ₁₄ H ₂₁	73				77.9- 79.2
C ₅ H ₁₁	C ₆ H ₁₃	53.7	(61.7)	62.4- 63.1	67.8- 67.9	84.1- 84.4 ³
C ₅ H ₁₁	C ₁₂ H ₂₅	52.2	(54.3- 54.4) ²	- -	69.6- 70.4	70.2- 70.6 ⁴

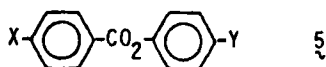
¹ Crystallization temperature at a cooling rate of 2°/min.

² () indicates a monotropic transition.

³ Previously reported by J. W. Goodby, *Liquid Crystals and Ordered Fluids*, Vol. 4, eds. A. C. Griffin and J. F. Johnson (Plenum Press, 1984), p. 175.

⁴ These two transitions overlap.

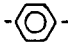



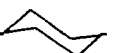



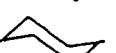
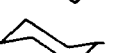

with the phenylbenzoates **5** as shown in Table VIII. Many of these phenylbenzoates gave INPs in mixtures with both the biphenyl **4a**



and the fluorene **4b** but with the latter more often, suggesting that the fluorene ring system, although not required, is more favorable for forming INPs than the biphenyl ring. Thus in some instances if an INP was observed in a mixture with the biphenyl compound, it was assumed it would also be observed with the fluorene compound. INPs were observed in many of the mixtures of both the biphenyl **4a** and the fluorene **4b** with the alkoxy halobenzoates **5** ($X = \text{RO}$, $Y = \text{halogen}$) (Nos. 20–36). However, there seems to be a combined alkoxy chain length and halogen size effect when $R = \text{C}_{10}$. INPs were observed when $Y = \text{F}$ (Nos. 35 and 36) but not when $X = \text{Cl}$ or Br (Nos. 37–40). Again it did not seem to matter on which end the halogen was attached (Nos. 43–50). Replacement of the alkoxy group with an alkyl group gave INPs only with the fluorene anil **4b** (Nos. 51–54). Again a chain effect was observed (Nos. 55–56).

These data definitely indicated that INPs could form in mixtures

TABLE V
Transition temperatures for

$X-\text{C}_6\text{H}_4-\text{O}_2\text{C}-\text{Y}-\text{CO}_2-\text{C}_6\text{H}_4-X$							
<u>X</u>	<u>Y</u>	<u>C</u> ¹	<u>S</u> ₄	<u>S</u> _B	<u>S</u> _C	<u>S</u> _A	<u>I</u>
C ₁₂ H ₂₅		128.7	- -	130.6- 131.5	139.8- 139.9	- -	143.0- 143.9
C ₈ H ₁₇		51.5	- -	70.3- 70.8	- -	114.3- 114.8	139.2- ² 139.6
C ₁₀ H ₂₁		51.2	- -	64.8- 65.7	- -	117.2- 117.7	134.6- 135.2 ²
C ₁₂ H ₂₅		57.0	- -	68.6- 68.9	- -	119.2- 119.4	130.7- 131.8
C ₇ H ₁₅ O		88	95	96	107	111	180 ³
C ₈ H ₁₇ O		86	91	93	111	119	178 ³
C ₁₀ H ₂₁ O		83.6	83.8	87	111	146	170 ³
C ₁₂ H ₂₅ O		84	- -	90	112	156	163 ³
C ₁₄ H ₂₈ O		86	- -	94	114	155	156 ³
C ₁₆ H ₃₃ O		90	- -	96	114	- -	150 ³
C ₁₈ H ₃₇ O		94.9	- -	113.3- 114.6	114.2- 115.1	- -	143.0- 144.0

¹ Crystallization temperature at a cooling rate of 2°/min.

² Data from M. E. Neubert, M. E. Stahl, and R. E. Cline, *Mol. Cryst. Liq. Cryst.* **89**, 93 (1982).

³ Data from M. E. Neubert, J. P. Ferrato, and R. E. Carpenter, *Mol. Cryst. Liq. Cryst.* **53**, 229 (1979).

with the halo phenylbenzoates but was the halogen atom really necessary? Unfortunately most of the phenylbenzoates with alkyl and alkoxy substituents have nematic phases. This is also true of the anils and limited the homologs of either of these series which could be used for mixture studies. One exception among the esters is $X = \text{C}_6\text{H}_{13}$ and $Y = \text{OCH}_3$. An INP was observed with this compound when it was mixed with the biphenyl **4a** (No. 19). INPs were also

TABLE VI
Transition temperatures (°C)* for

<u>R</u>	<u>S_H</u>	<u>S_G</u>	<u>S_F</u>	<u>S_I</u>	<u>S_C</u>	<u>S_A</u>	<u>I</u>
C ₈ H ₁₇	(46)	63.5	138.5	- -	156.8	197.5	202.5
C ₁₀ H ₂₁		72.3	115	148.7	154.8	189.2	191

* Data from A. Wiegeleben, L. Richter, J. Deresch, and D. Demus, *Mol. Cryst. Liq. Cryst.* **59**, 329 (1980).

observed in the two analogs containing only one alkoxy group ($X = C_4H_9O$ and $Y = H$; $X = H$, $Y = C_4H_9O$) but only when mixed with the fluorene compound **4b** (Nos. 15–18). As with the anils, it did not matter to which end the alkoxy group was attached. However, the ester with no terminal substituents ($X = Y = H$) did not give INPs either with the biphenyl or the fluorene compounds (Nos. 13 and 14).

The polarity of the terminal substituents is considered to be an influencing factor in the formation of induced S_A phases^{20,21} and such electron attracting groups as NO_2 and $C\equiv N$ are known to favor the formation of nematic phases. Thus mixtures of the nitro ester in which $X = C_{10}H_{21}O\ddagger$ and $Y = NO_2$ with both the biphenyl and fluorene compounds were tried but no INPs were observed (Nos. 41 and 42) suggesting that a strong polar substituent is undesirable for forming INPs.

Would the branched chain effect observed earlier in the phenylbenzoates²³ also occur in these mixtures i.e. would INPs be observed in mixtures with a β -methyl alkyl chain ester but not with an α -methyl one? The β -methyl esters gave INPs with both the biphenyl **4a** and fluorene **4b** anils (Nos. 67–72) whereas the α -methyl esters gave INPs with only the fluorene anil **4b** (Nos. 59–66). These results suggest that there is enough room to pack the thicker α -methyl ester molecules between the fluorene molecules but not between the biphenyl ones. Of the three structures being considered here, it would seem that the fluorene anil would have the largest diameter and the resulting larger molecular volume would be better able to accom-


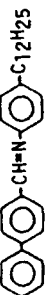

$\ddagger X \approx C_4H_9O$ has a monotropic nematic phase (see Ref. 22).

TABLE VII
Induced nematic phases in binary mixtures of short chloro anils with long biphenyl or fluorene anils

		with		INP	
				or	
X	Y	S	+		+
H	Cl	0	1.	0	2. +
CH ₃ O	Cl	0	3.	+	4. +
C ₄ H ₉ O	Cl	+	5.	+	6. +
C ₈ H ₁₇ O	Cl	+	7.	0	8. 0
F	Cl	0	9.	+	10. +
Cl	CH ₃ O	0	11.	+	12. +

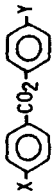


S = smectic phases in components: + observed, 0 not observed
INP = induced nematic phase: + observed; 0 not observed

TABLE VIII
Induced nematic phases in binary mixtures of short phenyl benzoates with long biphenyl or fluorene anils

		with		INP			
X	Y	S	+		or		+
H	H	0	13.	0		14.	0
C ₄ H ₉ O	H	0	15.	0		16.	+
H	C ₄ H ₉ O	0	17.	0		18.	+
C ₆ H ₁₃	OCH ₃	0	19.	+		-	-
C ₄ H ₉ O	F	0	20.	+		21.	+
	Cl	0	22.	+		23.	+
	Br	0	24.	+		25.	+
C ₆ H ₁₃ O	F	+	26.	+		-	-
	Cl	0	27.	+		28.	+
	I	0	29.	+		30.	+

C ₈ H ₁₇ O	F	+	31. +	32. +
	Cl	+	33. +	34. +
C ₁₀ H ₂₁ O	F	+	35. +	36. +
	Cl	+	37. 0	38. 0
	Br	+	39. 0	40. 0
	NO ₂	+	41. 0	42. 0
F	OC ₆ H ₁₃	0	43. +	44. +
I	OC ₆ H ₁₃	0	45. +	46. +
F	OC ₁₀ H ₂₁	0	47. +	48. +
I	OC ₁₀ H ₂₁	0	49. 0	50. 0
C ₄ H ₉	F	0	51. 0	52. +
C ₆ H ₁₃	I	0	53. 0	54. +
C ₁₀ H ₂₁	I	0	55. 0	56. 0

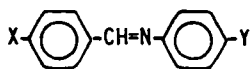
TABLE VIII continued

					
X	Y	S	+		+
Me ₂ CH- EtCH(Me)-	OCH ₃	0	57. 0		58. +
	OCH ₃	0	59. 0		60. +
	OC ₃ H ₇	0	61. 0		62. +
	OC ₆ H ₁₃	0	63. 0		64. +
	OC ₈ H ₁₇	0	65. 0		66. +
Me ₂ CHCH ₂	OCH ₃	0	67. +		68. +
	OC ₂ H ₅	0	69. +		70. +
	OC ₃ H ₇	0	71. +		62. +

S = smectic phases in components: + observed, 0 not observed
INP = induced nematic phase: + observed; 0 not observed

moderate the bulky α -methyl chain. However, an approximate measurement of the diameters of these molecules using Ealing CPK molecular models indicated that the biphenyl anil has the largest diameter (see Table IX). If the well known fact that molecules always pack in the most efficient manner leaving as little blank space as possible is considered then a possible explanation can be provided. The diameter of the α -methyl ester is the same as the straight chain analog. However, it is thicker at the α -carbon atom than anywhere in the rest of the molecule i.e. it has a hump. Where there is a hump, there is also an adjacent hole. This is true of the fluorene anil molecule which has its hump, although smaller, at the methylene carbon in the fluorene ring. Thus these two molecules could pack in a lock and key manner which allows the humps to fit into the holes. However, this does not explain why no mesophases are observed in the α -methyl esters themselves. In the fluorene compound, the hump is near the end of the molecule whereas in the ester, it is near the center. Perhaps a better packing arrangement is possible with this combination rather than all the molecules having their humps near the center. The fluorene anil itself shows smectic phases although no nematic phases indicating that it is at least more favorable for forming mesophases than the α -methyl phenylbenzoate which shows no mesophases at all. Perhaps the packing between these two different molecules is more favorable for forming a nematic phase in the mixture but not in the two separate components.

Since the earlier work on INPs in mixtures of FC12A and 40.Cl had suggested that INPs would be favored by two components with considerably different molecular lengths⁹ all the mixtures studied thus far consisted of a relatively long molecule **4a** or **4b** and a relatively short one. A variety of other long molecules were tried as possible substitutes for the biphenyl and fluorene compounds as shown in Table X. First to be considered was whether the biphenyl ring system was needed. Various mixtures with the corresponding benzene anil **4c** were tried but none of these showed INPs (Nos. 73–77) suggesting that the biphenyl is a necessary structural feature. However, adding a terminal fluorine to this molecule **6a** gave INP's with the chloro anils (Nos. 78 and 79) and with a phenylbenzoate (No. 80) suggesting



6a X = F, Y = C₁₂H₂₅

b X = H, Y = C₂H₅

that the biphenyl ring system is not necessary but perhaps more

TABLE IX
Molecular dimensions of mixture components¹

Component	X or Ar	Y	Molecular Length (Å)	Molecular Diameter (Å)	Molecular Thickness (Å)
	H	C ₂ H ₂₅	15.5	6.7	3.6
	H	C ₁₂ H ₂₅	27.8	6.7	
	H	Cl	14.7	6.7	
	or	Cl	15.9	6.7	
		CH ₃ O			
	Cl	Cl	20.1 ²	6.7	
	C ₄ H ₉ O	Cl	25.0	6.7	
	C ₈ H ₁₇ O	Cl	15.5	6.7	
	F	Cl	28.5	6.7	
	F	C ₁₂ H ₂₅			
	H	H	13.2	6.7	
	C ₄ H ₉ O	H	18.4	6.7	
	or	C ₄ H ₉ O			5.1
		H			
	C ₆ H ₁₄	C ₄ H ₉ O	22.2	6.7	
	C ₄ H ₉ O	OCH ₃	19.1	6.7	
	C ₄ H ₉ O	Cl	19.9	6.7	
	C ₄ H ₉ O	Pr	20.4	6.7	
	C ₆ H ₁₃ O	F	21.8	6.7	
	C ₆ H ₁₃ O	Cl	22.4	6.7	
	C ₆ H ₁₃ O	I	23.4	6.7	
	C ₈ H ₁₇ O	F	24.2	6.7	
	C ₈ H ₁₇ O	Cl	25.1	6.7	
	C ₈ H ₁₇ O	Cl	25.1	6.7	

[illegible]

TABLE IX continued

Component	X or Ar	Y	Molecular Length (Å)	Molecular Diameter (Å)	Molecular Thickness (Å)
	C ₈ H ₁₇	-	38.0	7.4	5.2
	C ₁₀ H ₂₁	-	42.0	7.4	
	C ₁₂ H ₂₅	-	47.4	7.4	
	C ₇ H ₁₅ O	-	36.9	7.4	
	C ₈ H ₁₇ O	-	39.4	7.4	
	C ₁₀ H ₂₁ O	-	43.8	7.4	
	C ₁₄ H ₂₉ O	-	48.2	7.4	
	C ₁₆ H ₃₂ O	-	52.6	7.4	
	C ₁₈ H ₃₇ O	-	61.4	7.4	
	C ₈ H ₁₇	-	38.4	8.4	3.6
	C ₁₀ H ₂₁	-	43.5	8.4	
	C ₁	-	19.05	7.3	
	C ₁₂ H ₂₅	-	32.2	7.3	
	C ₁₂ H ₂₅	-	31.6 ³	6.8	
	C ₁₂ H ₂₅	-	29.9	9.0	
	C ₁₂ H ₂₅	-	29.9	9.0	
	C ₁₂ H ₂₅	-	29.9	9.0	

¹ Measured on Ealing CPK molecular models using the most extended configuration.
² The molecular length of this molecule has been determined by x-ray diffraction to be 20.7 Å (see Ref. 9).
³ The molecular length of this molecule has been determined by x-ray diffraction to be 32.4 Å (see Ref. 9).

TABLE X
Induced nematic phases (INP) in mixtures containing long and short molecules

Long Molecule	Short Molecule	λ	S	INP	
		\underline{R}			
		73. C ₄ H ₉	0	+	0
		74. C ₈ H ₇	0	+	0
		\underline{Y}			
		\underline{X}			
		75. C ₄ H ₉ O	0	0	0
		76. Me ₂ CHCH ₂			
		77. C ₄ H ₉ O	0	0	0
		\underline{R}			
		78. C ₄ H ₉	0	+	+
		79. C ₈ H ₁₇	0	+	+
		\underline{Y}			
		\underline{X}			
		80. C ₆ H ₁₃	0	0	+
		81. C ₄ H ₉ O	0	0	0
		\underline{Y}			
		\underline{R}			
		82. C ₄ H ₉	0	+	0
		83. C ₈ H ₇	0	+	0
		\underline{Y}			
		\underline{X}			
		84. C ₆ H ₁₃	0	0	+
		85. C ₄ H ₉ O	0	0	+
		\underline{Y}			

TABLE X continued

Long Molecule	Short Molecule	λ	S	INP
	86.	+	0	+
	87.	0	+	+
	88.	0	0	+
	$X-\text{C}_6\text{H}_4-\text{CO}_2-\text{C}_6\text{H}_4-\text{Y}$			
	\underline{X}			
	89. $\text{C}_4\text{H}_9\text{O}$	0	0	+
	90. C_6H_{13}	0	0	+
	91. $\text{EtCH(Me)}-\text{OCH}_3$	0	0	+
	92. $\text{Me}_2\text{CHCH}_2-\text{OCH}_3$	0	0	+
	93. $\text{C}_4\text{H}_9\text{O}$	0	0	+
	94. $\text{C}_6\text{H}_{13}\text{O}$	0	0	+
	\underline{Y}			
	\underline{R}			
$\text{CH}_3\text{O}-\text{C}_6\text{H}_4-\text{CO}_2\text{R}'$	R'			
	C_4H_9	+	0	++
	95. CH_3	+	+	0
	96. $\text{C}_4\text{H}_9\text{O}$	+	+	0
	97. $\text{C}_8\text{H}_{17}\text{O}$	+	+	0
	98.	+	0	0





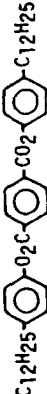




C_6H_{13}		\underline{R} 99. CH_3 100. C_4H_9 101. C_8H_{17}	+	0	+
	\underline{X}	102. $EtCH(Me)-$ 103. C_4H_9O	+	0	0
	\underline{Y}	104. CH_3 105. C_4H_9 106. C_8H_{17}	0	0	0
$C_{14}H_{29}$		\underline{R} 107. $EtCH(Me)-$ 108. C_4H_9O 109. $C_8H_{17}O$	0	0	0
	\underline{X}	110. CH_3 111. C_4H_9	0	0	0
	\underline{Y}		0	0	0
$C_5H_{11}O-CO_2R$		\underline{R} 110. CH_3 111. C_4H_9	+	0	0
C_6H_{13}			+	0	0

TABLE X continued

Long Molecule	Short Molecule	Σ	S	INP
$C_{12}H_{25}$		\underline{R}	+	+
		113. CH_3	+	+
		114. C_4H_9	+	+
		115. C_8H_{17}	+	0
		116. C_4H_9	+	+
		117. C_8H_{17}	+	+
$C_{12}H_{25}$		\underline{R}	+	0
		118. CH_3	+	+
		119. C_4H_9	+	+
		120. C_4H_9	+	+
		121. C_8H_{17}	+	+
\underline{Z}		\underline{Y}	+	+
C_8H_{17}		\underline{X}	+	+
		122. CH_3O	+	+
		123. C_4H_9O	+	+
		124. $C_8H_{17}O$	+	0
		125. F	+	+
		\underline{R}	+	+
$C_{10}H_{21}$		127. C_4H_9	+	+
		128. C_8H_{17}	+	0






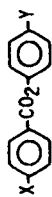

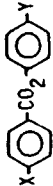

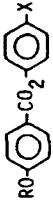
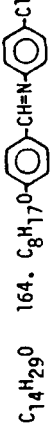
$C_{12}H_{25}$		129. $C_8H_{17}O-C_6H_4-CO_2-C_6H_4-F$	+	+	+
		130. C_4H_9 131. C_8H_{17}	+	+	+
			+	+	0
$C_7H_{15}O$		132. $C_8H_{17}O-C_6H_4-CO_2-C_6H_4-F$	+	+	+
$C_7H_{15}O$		133. $C_8H_{17}O-C_6H_4-CH=N-C_6H_4-Cl$	+	+	+
$C_8H_{17}O$		\underline{R} 134. C_4H_9 135. C_8H_{17}	+	+	+
		\underline{X} \underline{Y}	+	+	+
		136. $EtCH(Me)-OMe$	+	0	0
		137. Me_2CHCH_2OMe	+	0	+
		138. C_4H_9O	+	0	+
		139. $C_8H_{17}O$	+	+	+
		140. $C_{10}H_{21}O$	+	+	+
		141. $C_6H_{13}O$	+	0	+
		142. $C_8H_{17}O$	+	+	+
		143. $C_{10}H_{21}O$	+	+	0
		144. $C_{10}H_{21}O$	+	+	0
			+	+	0
$C_{10}H_{21}O$		\underline{R} 145. C_4H_9 146. C_8H_{17}	+	+	+
			+	+	+

TABLE X continued

Long Molecule	Short Molecule	S			
		L	S	INP	
		<u>X</u>	<u>Y</u>		
		147. EtCH(Me)-	OC ₃ H ₇	+	0
		148. Me ₂ CHCH ₂ -	OCH ₃	+	0
		149. C ₄ H ₉ O	F	+	0
		150. C ₈ H ₁₇ O	F	+	+
		151. C ₁₀ H ₂₁ O	F	+	+
		152. C ₆ H ₁₃ O	Cl	+	0
		153. C ₈ H ₁₇ O	Cl	+	+
		154. C ₁₀ H ₂₁ O	Cl	+	0
		155. C ₁₀ H ₂₁ O	Br	+	0
		156. C ₁₀ H ₂₁ O	NO ₂	+	0
				+	+
		<u>R</u>	<u>X</u>		
		158. C ₈ H ₁₇	F	+	+
		159. C ₁₀ H ₂₁	F	+	+
		160. C ₆ H ₁₃	Cl	+	0
		161. C ₈ H ₁₇	Cl	+	+
		162. C ₁₀ H ₂₁	Cl	+	0
		163. C ₁₀ H ₂₁	Br	+	0
				+	+

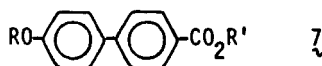
Long Molecule	Short Molecule	S
C ₁₈ H ₃₇ O	181. CH ₃ O-C ₆ H ₄ -CH=N-C ₆ H ₄ -Cl	+ 0 +
	182. C ₈ H ₁₇ O-C ₆ H ₄ -CH=N-C ₆ H ₄ -Cl	+ + +
	X-C ₆ H ₄ -CO ₂ -C ₆ H ₄ -Y	
	X Y	
	183. EtCH(Me)-OCH ₃	+ 0 0
	184. C ₈ H ₁₇ O F	+ + +
	185. C ₈ H ₁₇ O Cl	+ + +
	186. C ₁₀ H ₂₁ O Cl	+ + +
	187. C ₁₀ H ₂₁ O Br	+ + +
	188. C ₁₀ H ₂₁ O NO ₂	+ + 0
R'	R	
C ₈ H ₁₇	RO-C ₆ H ₄ -CH=N-C ₆ H ₄ -Cl	+ + +
C ₁₀ H ₂₁		+ + 0
		+ + +
		+ + 0

INP in mixture: + observed, 0 not observed.

favorable and that the halogen atoms are more favorable than hydrogen. The next feature studied was the alkyl chain length. Unfortunately, the observance of nematic phases in most of the biphenyl anil homologs limited the choices to the very short chain lengths. The ethyl homolog **6b** gave INPs when mixed with the phenylbenzoates (Nos. 84 and 85) but not with the chloro anils (Nos. 82 and 83). This ethyl homolog could also be considered a short molecule so it was mixed with the fluorene anil **4b** and found to form an INP (No. 86).

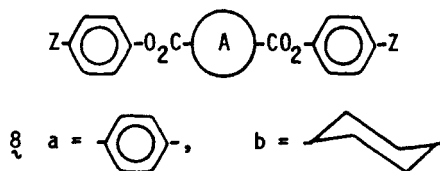
INPs were observed in all the mixtures tried with the naphthalene anil **4d** (Nos. 87–94). Although no nematic phase was observed in this compound (**4d**) during a routine determination of its transition temperatures, a phase diagram study (to be discussed later) suggested the presence of a monotropic nematic phase. This was then observed briefly when a melt of the sample was placed on the heating stage at ca. 40°. Thus the nematic phases observed in mixtures with this compound cannot necessarily be considered as INPs.

Other long molecules which did not resemble the anils **4** in their structure were also considered (Table X). INPs were observed in some of the mixtures with the alkoxybiphenyl esters **7**. Although no



effort was made to look for induced smectic phases in these mixtures, one was observed in the mixture of the biphenyl **7** with $R = \text{CH}_3$ and $R' = \text{C}_4\text{H}_9$ (No. 95) along with an INP. Although these biphenyl esters did not seem to be as favorable for forming INPs as the biphenyl and fluorene anils, the observance of some INPs with these compounds did indicate that none of the structural features of FC12A are required in the long component to observe INPs.

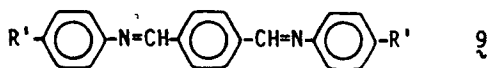
Diesters of the type **8** are even longer molecules than the anils **4a** and **b**. INPs were observed in mixtures of short compounds with both



the terephthalic acid diesters **8a** (Nos. 119–121) and the cyclohexanes **8b** (see Table X). As with the anils **4a** and **b** chain effects were also

observed with the cyclohexane diesters.[†] However, these seemed to depend on the structure of the short molecule as well as the cyclohexane diesters' substituent. When Z was an alkyl substituent (C₈, C₁₀, or C₁₂), INPs were observed with the shorter chain alkoxy chloro anils (Nos. 122, 123, 127, and 130) but not when the alkoxy group was C₈ (Nos. 124, 128 and 131). When Z = R'O, INPs were observed in mixtures with the chloro anils at all chain lengths of R' (Nos. 133–135, 145, 146, 157, 164, 174, 181, and 182) with all the anils studied. In mixtures with the halo phenylbenzoates, there seemed to be a combined halogen-chain length effect when Z = R'O. When X was < C₁₀O, Y could be F or Cl and INPs were observed for any R' chain length but when X = C₁₀, Y could be only F when R' was < C₁₆. However, when R' was C₁₆ or larger, INPs were observed even when Y = Br (Nos. 180 and 187).

Like the biphenyl anil, the cyclohexane diesters with Z = R'O did not form INPs with the α-methyl chain phenylbenzoates no matter how long the R' group became (Nos. 136, 147, 165, and 183) but did form INPs with the β-methyl esters (Nos. 137, 148, and 166). A comparison of the molecular diameters of the cyclohexane diesters with that for the phenylbenzoates using molecular models indicates that the cyclohexane esters have a slightly larger diameter (see Table IX). This apparently is not enough to accommodate the thick α-methyl phenylbenzoate or there is not a proper hump-cavity to accommodate the one in the α-methyl phenylbenzoate. The dianils **9** also gave INPs when mixed with the chloro anils (Nos. 189 and 191)



but only when R = C₄ and not when R = C₈ again suggesting a chain length effect.

With such long molecules which were so different in structure from that for FC12A showing INPs, it seemed necessary to determine if the original assumption that two molecules with a significant difference in molecular length was needed was correct. This was supported by the finding of several papers in a literature search reporting the observance of INPs in mixtures of two homologs.^{3,4,7} Therefore, three types of mixtures were studied to try to determine what types of molecular lengths were needed to observe INPs; two homologs (Table

[†] We did not have enough of the terephthalic acid ester homologs to study the chain effect on these.

TABLE XI




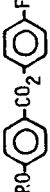
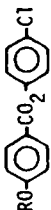
Induced nematic phases in binary mixtures of homologs

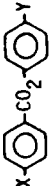
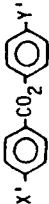
Compound	n	S ¹	INP ²
$C_nH_{2n+1}O-\text{C}_6\text{H}_4-\text{CH}=\text{N}-\text{C}_6\text{H}_4-\text{Cl}$	193. 1+4	+	+
	194. 1+8	+	+
	195. 4+8	+	+
$\text{C}_6\text{H}_5-\text{CH}=\text{N}-\text{C}_6\text{H}_4-\text{C}_nH_{2n+1}$	196. 2+12	0	+
$X-\text{C}_6\text{H}_4-\text{CO}_2-\text{C}_6\text{H}_4-Y$			
X	Y		
197. EtCH(Me)-	OC_nH_{2n+1}	3+6	0 0 0
198. Me_2CHCH_2-	OC_nH_{2n+1}	1+3 ³	0 0 +
$C_nH_{2n+1}O$	F	199. 4+8	0 + +
		200. 4+10	0 + +
		201. 8+10	+
	Cl	202. 6+8	0 + 0
		203. 6+10	0 + 0
		204. 8+10	+
$RO-\text{C}_6\text{H}_4-\text{C}_6\text{H}_4-\text{CO}_2C_nH_{2n+1}$	R		
	205. CH_3	4+6	+
	206. C_5H_{11}	6+12	+
$X-\text{C}_6\text{H}_4-O_2C-\text{C}_6\text{H}_{10}-CO_2-\text{C}_6\text{H}_4-X$	X		
	207. C_nH_{2n+1}	8+10	+
	208. $C_nH_{2n+1}O$	8+10	+
	209. $C_nC_{2n+1}O$	8+16	+
	210. $C_nH_{2n+1}O$	8+18	+

¹ S = smectic phases in components: + present, 0 not observed.² INP = induced nematic phase: + observed; 0 not observed.³ n = 6 has a nematic phase.

XI); two short molecules which are not homologs (Table XII), and two long molecules (Table XIII). Any combination of two homologs of the various chloro anils used in this work gave INPs (Nos. 193–195). A mixture of the C_2 and C_{12} homologs of the biphenyl anil gave an INP (No. 196) as did various combinations of the alkoxy-fluorophenylbenzoates (Nos. 199–201). Interestingly, various combinations of the alkoxy chloro phenylbenzoates did not form INP's (Nos. 202–204). The combination of a straight chain phenylbenzoate with a β -methyl branched chain one gave an INP (No. 198) but the analogous mixture with the α -methyl branched chain ester did not (No. 197). Neither the biphenyl esters (Nos. 205 and 206) or the cyclohexane

TABLE XII
Induced nematic phases in binary mixtures containing two short molecules







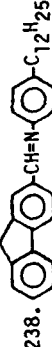


Component A	Component B	S ¹					
		A	B	INP ²			
		<u>X</u> F	R	0	+	0	
				211. C ₄ H ₉	0	+	0
				212. C ₈ H ₁₇	0	+	0
CH ₃ O	213. 			0	0	0	
C ₄ H ₉ O				214. C ₄ H ₉	+	0	+
				215. C ₄ H ₉	+	+	+
				216. C ₆ H ₁₃	+	+	+
				217. C ₈ H ₁₇	+	+	+
				218. C ₁₀ H ₂₁	+	+	+
C ₈ H ₁₇ O				219. C ₄ H ₉	+	0	+
				220. C ₈ H ₁₇	+	+	+
				221. C ₁₀ H ₂₁	+	+	0
			<u>R</u>	222. C ₆ H ₁₃	+	0	+
C ₄ H ₉ O				223. C ₈ H ₁₇	+	+	+
				224. C ₁₀ H ₂₁	+	+	+

	\underline{X}	\underline{Y}		$\underline{X'}$	$\underline{Y'}$	225. C_6H_{13}	+	0	0
C_4H_9O		H		228. H	OC_4H_9				
$C_{10}H_{21}O$		F		229. $C_{10}H_{21}O$	Br		+	+	0
		Cl		230. $C_{10}H_{21}O$	F		+	+	0
		Cl		231. $C_{10}H_{21}O$	Br		+	+	0
						226. C_8H_{17}	+	+	0
						227. $C_{10}H_{21}$	+	+	0

¹ S = smectic phases in components: + observed, 0 not observed.

² INP = induced nematic phase: + observed, 0 not observed.

TABLE XIII
Induced nematic phases in binary mixtures containing two long molecules

Component A	Component B	S ¹			INP ²
		A	B		
	232. 	0	0	0	0
	233. 	0	+	0	0
	X- 	<u>X</u>			
	234. 	234. C ₈ H ₁₇	0	+	0
		235. C ₈ H ₂₁	0	+	0
		236. C ₁₀ H ₂₁	0	+	0
	237. 	+	0	+	+
	238. 	+	+	+	0
	239. 	+	+	+	+
	240. 	+	+	+	0





	\underline{X}			
	241. C_8H_{17}	+	+	0
	242. $C_{12}H_{25}$	+	+	0
	243. $C_8H_{17}O$	+	+	+
	244. $C_{10}H_{21}O$	+	+	+
	245. $C_{18}H_{27}O$	+	+	+
		+	+	0
	246. C_8H_{17}			
	247. F			
	248. CH_3O			
	249. $C_5H_{11}O$			
	X			
				
	250. C_8H_{17}	+	+	0
	251. $C_{12}H_{25}$	+	+	0
	252. $C_8H_{17}O$	+	+	+
		+	+	0
	253. C_8H_{17}			

TABLE XIII continued

Component A	Component B	S ¹			
		A	B	INP ²	
		+	0	0	0
		+	+	0	0
		+	0	+	+
		+	+	0	0
		+	+	0	0

¹ S = smectic phases in components: + observed, 0 not observed.

² INP = induced nematic phase: + observed; 0 not observed.

diesters (Nos. 207–210) gave INPs in homologous mixtures. With the biphenyl esters, we were limited by the availability of the materials whereas with the cyclohexane diesters we were limited to using only the longer chain lengths ($>C_7$) as the shorter ones have nematic phases. INPs might be more favored in mixtures of shorter chain homologs.

Interestingly, among the mixtures of two short molecules which were not homologs (Table XII) only mixtures of the chloro anils **1** with the halo phenyl benzoates **2b** ($X = F, Cl$) showed INPs (Nos. 214–220 and 222–224). Mixtures of anils with anils (Nos. 211–212) or esters with esters containing two different halogens (Nos. 228–231) did not form INPs. The anil-ester mixtures also showed a combined chain-length, halogen size effect as shown by the absence of INPs when $X = C_8H_{17}O$ and $R = C_{10}H_{21}$ in the fluoro ester (No. 221) and when $X = C_8H_{17}O$ and $R = C_6-C_{10}$ in the chloro esters (Nos. 225–227).

In the mixtures with two long molecules (Table XIII), combinations of the biphenyl anil **4a** with the phenyl anil **4c** (No. 233), the fluorene anil **4b** (No. 238) and a TBBA homolog **9** ($R' = C_8$) (No. 246) showed no INPs whereas one was observed with the fluoro anil **6a** $Y = F$ (No. 237). INPs were observed in mixtures of either the biphenyl anil **4a** or the fluorene anil **4b** but not the phenyl anil **4c** with the cyclohexane diesters **8b** when Z is an alkoxy substituent (Nos. 235, 236, 243–245, and 252) but not when $Z = \text{alkyl}$ (Nos. 234, 241, 242, 250, and 251). INPs were not observed in mixtures with the longer chain biphenyl ester **7** ($R = C_5H_{11}$ and $R' = C_{12}H_{25}$) (Nos. 240 and 249). Nor were INPs observed in mixtures of the alkyl cyclohexane diesters with the fluoro anil (No. 254) an alkoxy cyclohexane diester (Nos. 255 and 258) or a terephthalic acid diester (No. 257). However, an INP was observed with the fluoro anil **6a** (No. 256). From these data, it appears that INPs can occur but are not as favored in mixtures of two long molecules. The presence of an INP in the mixture of the fluorene anil with the short chain biphenyl ester might be because the biphenyl is really a short molecule. A comparison of molecular lengths obtained by measuring molecular models is presented in Table IX. The molecular lengths for all the molecules that have been considered short in this discussion are $<30 \text{ \AA}$. This also is true of the short chain biphenyl ester **7** ($R = CH_3$, $R' = C_6H_{13}$) and the fluoro anil **6a** which would explain why an INP was observed in mixtures of the fluorene and biphenyl anils with these compounds. No INP was observed in analogous mixtures with the longer chain biphenyl ester **7** ($R = C_5H_{11}$ and $R' = C_{12}H_{25}$) (Nos. 240 and 249) which has

a molecular length >30 Å. The phenyl anil **4c** could also then be considered a short molecule as well. It did not form INPs with short molecules (see Table X) and obviously does not with long ones either. Molecular length, however, does not explain why INPs were observed in mixtures of the biphenyl or fluorene anils with the alkoxy cyclohexane diesters (Nos. 243–245 and 252) but not with the analogous alkyl compounds. The difference between the molecular length of the C_8O cyclohexane diesters and the biphenyl anil might be enough to consider the biphenyl anil a short molecule compared to the cyclohexane ester. However, this would also be true of the C_{12} alkyl cyclohexane diester. One consistent trend among the mixtures of two long molecules is that INPs were not formed when both components were of near equal or equal lengths (Nos. 238, 255, 257, and 258) even with two homologs (Nos. 209 and 210).

Phase diagram†

A variety of mixture phase diagrams were obtained to determine which structural features gave better INPs. Problems were encountered in determining many of these diagrams due to poor mixing, mixed phase regions and transitions and monotropic phases. This was particularly true of the mixtures of the fluoro esters **1b** ($Y = F$) with the anils **4a** and **b**. Both enantiotropic and monotropic INPs were observed, sometimes within the same phase diagram. The only INP range which could be plotted for monotropic phases would be that between the NI and NC transitions. This is not practical since crystallization temperatures vary according to the conditions used. Mixtures containing one component with a smectic phase and the other without created two INP ranges, that between the CN and NI transitions and the one between the SN and NI transitions. Often a mixture of monotropic and enantiotropic phases were observed as well. Since our goal was to compare the widths of the INP ranges, these phase diagrams were simplified in two ways. Only mixtures in which both components containing at least one smectic phase were studied (Figure 4c is the exception) and only temperatures observed at the end of the SN and MI transitions were used. No differentiation was made between different smectic phases in the SN transitions.

A comparison of the INP region for mixtures of 40.Cl with the four major long molecules studied is presented in Figure 4. The INP range for most concentrations is larger for the fluorene anil **4b** (maximum

† C = crystal, S = smectic, N = nematic, I = isotropic, M = mesophase.

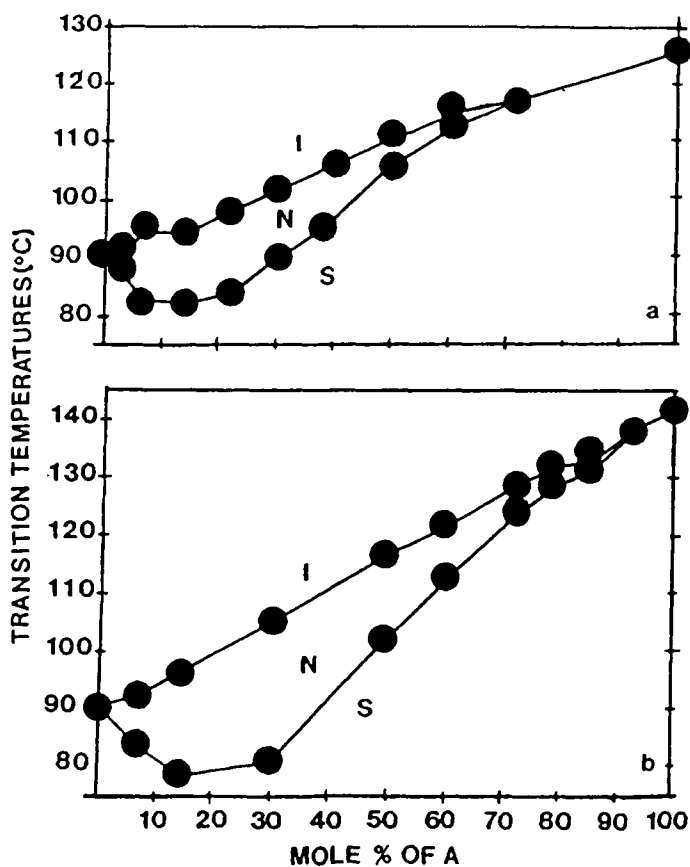
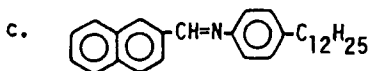
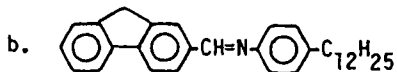
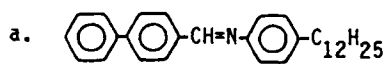


FIGURE 4 Phase diagrams for mixtures of

$C_4H_9O-C_6H_4-CH=N-C_6H_4-Cl$ with component A:



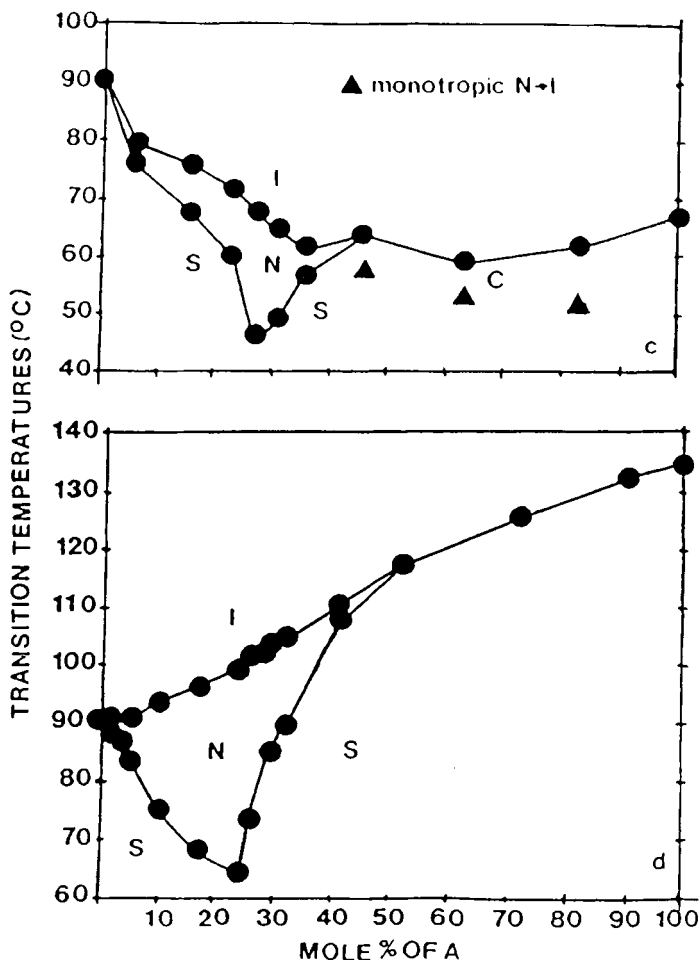
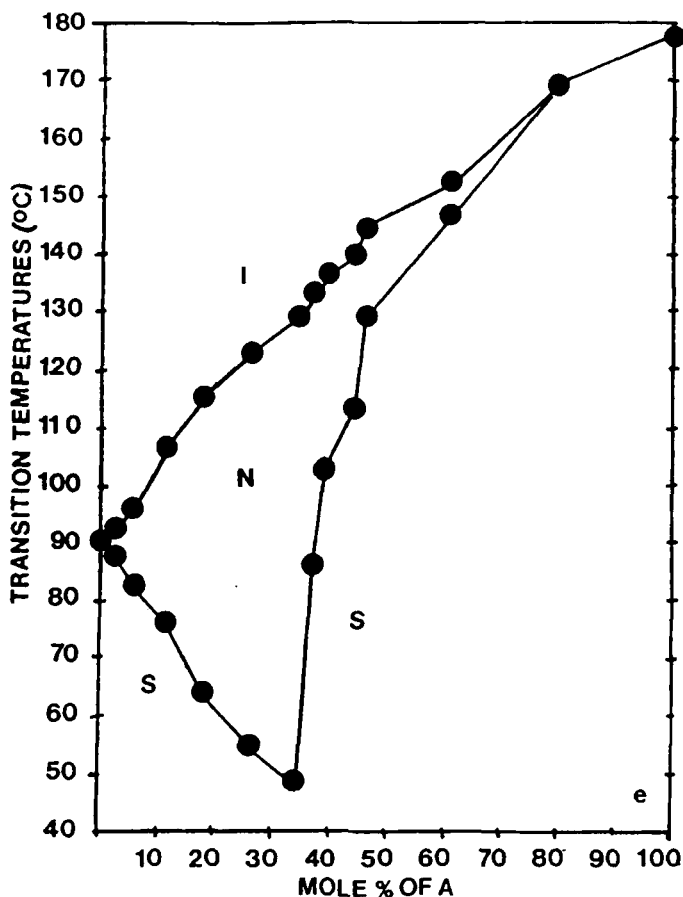


FIGURE 4 Continued

at $\sim 24^\circ$, Figure 4b) than for the biphenyl anil **4a** (maximum $\sim 12^\circ$, Figure 4a) suggesting that it is a better inducer. This is also supported by the existence of the INP over a wider concentration range for the fluorene anil mixtures. INPs were also observed over nearly the entire concentration range of the naphthalene anil **4d** mixtures (Figure 4c). The nematic phase however, was monotropic at concentrations of $>50\%$ of the naphthalene anil with no S_A below so that the INP region could not be plotted. The nematic-to-isotropic temperatures for these nematics decreased with increasing naphthalene anil con-

FIGURE 4 *Continued*

centrations suggesting that this compound should have a monotropic nematic phase. This was observed briefly before crystallization but only when a melted sample was placed on the heating stage at $\sim 42^\circ$ and allowed to cool rapidly. This explains why INPs were observed in all the naphthalene anil mixtures. Still the large INP range between 20 and 40% (maximum range = 21.7°) of the naphthalene anil and its persistence to low concentrations of this anil suggests that there is inducement of the nematic phase in this region.

A larger maximum INP range ($\sim 35^\circ$) was observed in the phase diagram (Figure 4d) for the dialkyl cyclohexane diester **8b** ($Z = C_{10}H_{21}$) mixtures than for the fluorene anils **4b** but the INP

occurred over a shorter concentration range; <50 mole % of the cyclohexane diester. A similar curve (Figure 4e) was observed for the analogous dialkoxy ester **8b** ($Z = C_8H_{17}O$) which showed an even larger maximum INP range ($\sim 80^\circ$). Some of this increase is probably due to the shorter alkyl chain but such a large increase also suggests an additional contribution by the alkoxy group. Interestingly, the larger INP ranges all occurred at concentrations of <50% of the long molecule in all these mixtures. This suggests that the shorter component has structural features more favorable for forming INPs than the longer component. The results obtained from the contact method suggest this also.

The phase diagram for mixtures of 2 homologs of the chloro anil **1** ($X = Cl$) showed an INP over only a short concentration range (~ 5 –40%) of the longer homolog and the INP range was very short (maximum = 1.0° , Figure 5). Mixtures of two short molecules having different structures also showed INPs over essentially the entire concentration range but with a longer INP range (maximum = 6.5° , Figure 6) suggesting that such mixtures favor INPs more than a mixture containing two short homologs. However, this INP range is not as wide as that observed for mixtures of short with long molecules. Although the shorter molecules appear to be more favorable for forming nematic phases, as would be expected, mixtures of a short with a long molecule seems to be needed to observe wide range INPs.

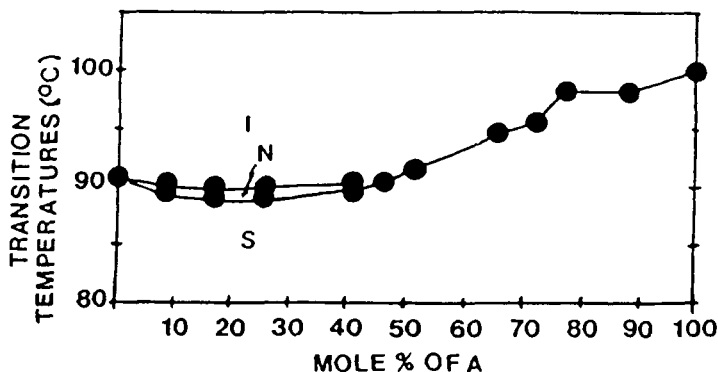
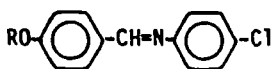


FIGURE 5 Phase diagram for a mixture of two homologs of



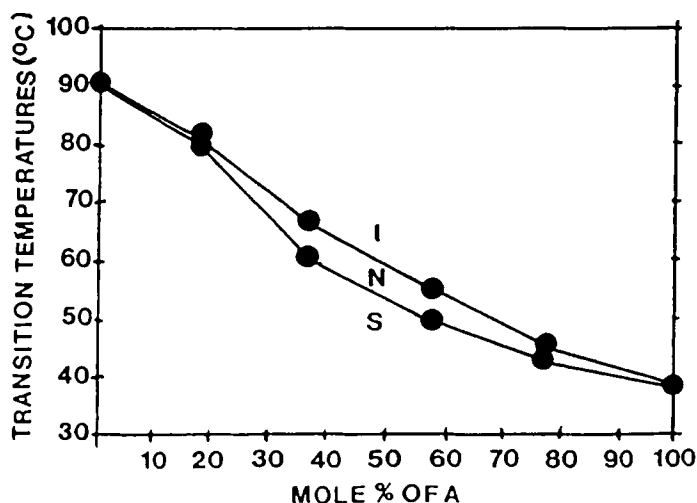
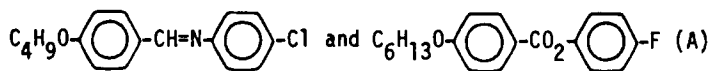


FIGURE 6 Phase diagram for a mixture of two short molecules:



In order to study the effect of chain length on INPs, phase diagrams were determined for mixtures of the fluoro esters **2b** ($X = F$) with both the fluorene anil **4b** (Figure 8) and the biphenyl anil **4a** (Figure 9). In the fluorene mixtures, INPs were observed essentially over the entire concentration range for the three homologs studied ($R = \text{C}_6$, C_8 , and C_{10}). In the mixtures with the C_6 homolog both with the fluorene (Figure 8) and biphenyl anils (Figure 9a), the SN transitions were difficult to observe in the 25–50% concentration range because these occurred below room temperature and near the crystallization point. The smectic phase could be observed only when the sample was cooled rapidly to lower the crystallization point. Since crystallization occurred too quickly to reheat the smectic phase to obtain the SN transition temperatures, the temperatures at which the smectic phase was observed on cooling are plotted. These are lower than the heating temperatures would be and therefore provide only an approximate curve of this minimum region. With the biphenyl anil mixtures (Figure 9a), crystallization occurred before the smectic phase could be observed at the minimum, but the falling trend was observed. A comparison of these curves for the different alkyl chain lengths of R illustrates that the range of the INP decreases with increasing chain length and that the INP is not as good with the biphenyl anils as with

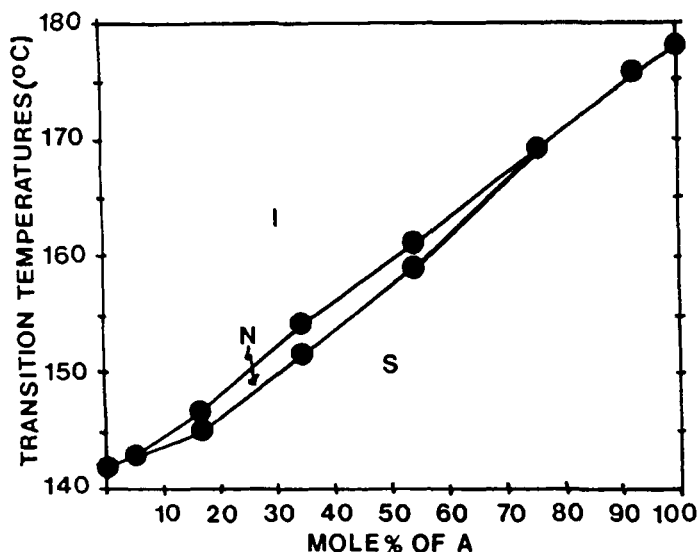
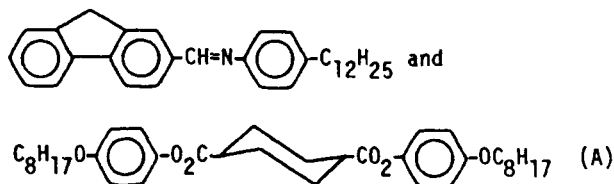


FIGURE 7 Phase diagram for a mixture of two long molecules:



the fluorene anils both in terms of composition and INP ranges. A similar effect was observed with increasing halogen size (Figures 8b and 10).

DISCUSSION

The screening of binary mixtures for INPs using the contact method provided the realization that a wide variety of components can be used to observe INPs. Little information was gained about what structural features favor formation of INPs or provide the longest range phases. The phase diagrams, on the other hand, provide a better means of differentiating between favoring structures, although not of specific structural features. These diagrams can be divided into two general types: those which show a narrow INP range between the nearby linear SN and MI curves without a minimum (Figures 5–7, 8b, 8c, 9b and c, and 10) and those which show large range INPs

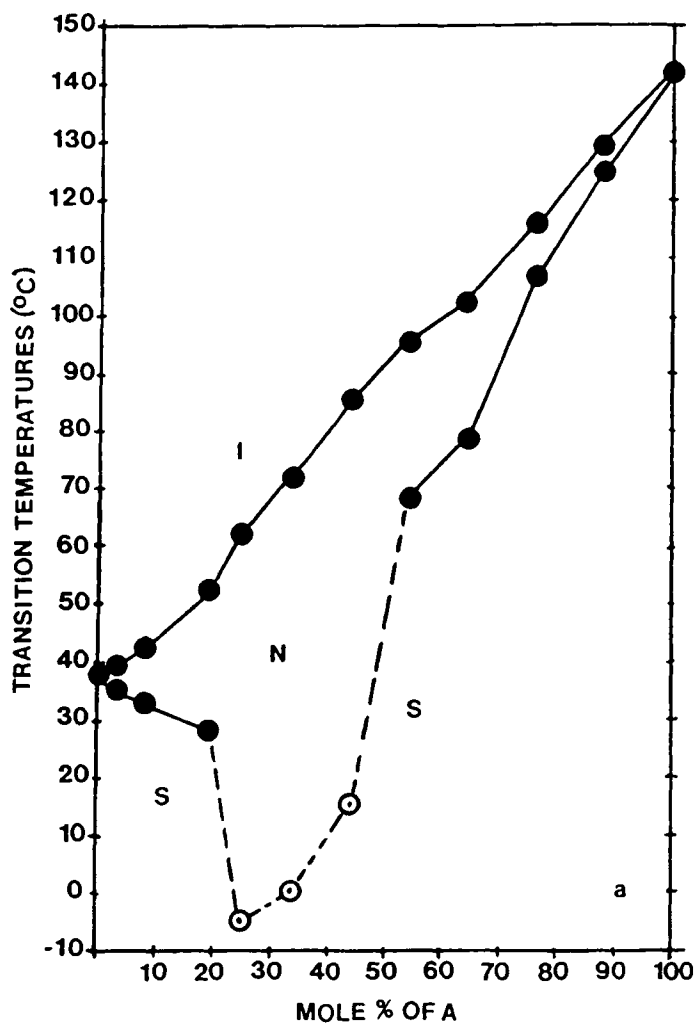
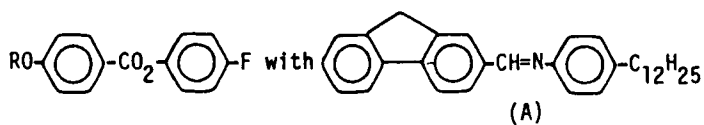
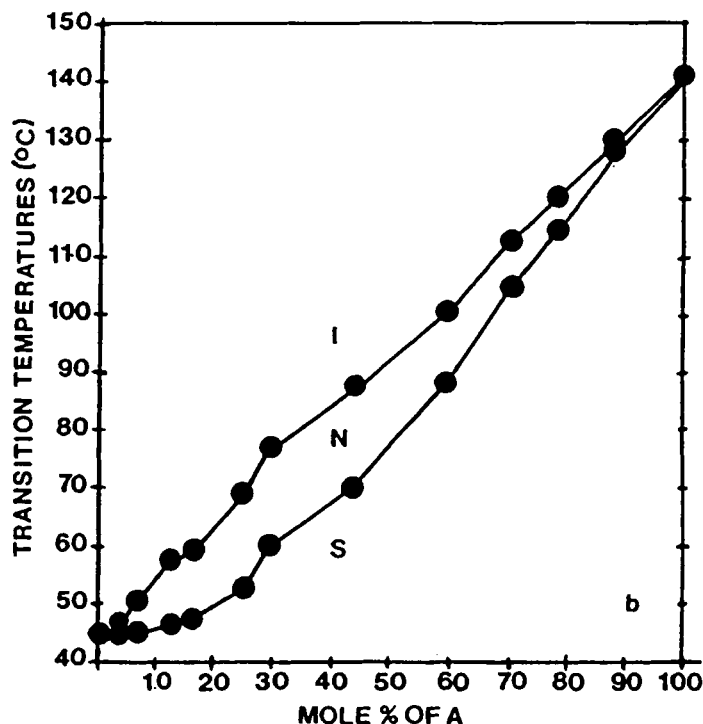


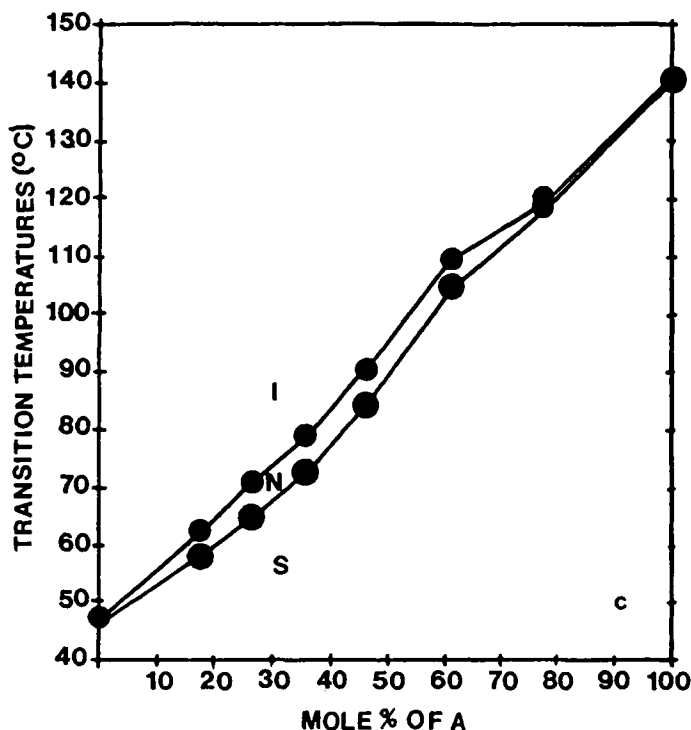
FIGURE 8 Phase diagrams for mixtures of



- a. $\text{R} = \text{C}_6\text{H}_{13}$
- b. $\text{R} = \text{C}_8\text{H}_{17}$
- c. $\text{R} = \text{C}_{10}\text{H}_{21}$

FIGURE 8 *Continued*

between a nearly linear MI curve and a non-linear SN curve with a minimum where the INP phases have their largest range (Figures 4, 8a, and 9a). Type I occurs in mixtures in which the molecules have similar molecular lengths which can either be short (Figures 5 and 6) or long (Figures 7, 8b and c, and 10), whereas Type II occurs only in mixtures in which the molecules differ considerably in molecular length (Figures 4, 8a, and 9a). To obtain some idea how large this difference must be to observe Type II curves, these differences are compared in Table XV. The smallest difference for a Type II curve which was studied is 9.8 and the largest difference for a Type I curve is 7.4 Å. These values are only approximate ones since they were determined by measuring molecular lengths on molecular models. Also there is a gap between these two for which data are needed but these data provide an indication of what this difference should be. A good example of the effect of this difference on the type of curve observed can be seen in the mixtures of either the fluorene or biphenyl anil with the homologous fluorine esters. Type I curves were observed

FIGURE 8 *Continued*

when $R = C_6$ (Figures 8a and 9a) but changed to Type II when $R = C_8$ or C_{10} (Figures 8b, 8c, 9b, and 9c).

These results are similar to those Dave and Dewar observed in binary mixtures which did not show INPs.²⁴ They found that in mixtures of molecules of similar molecular lengths, a plot of either the CI and/or MI transition temperatures (some components contained a nematic phase) versus concentration was essentially linear with no minimum whereas mixtures containing molecules of two different molecular lengths showed non-linear curves with a minimum. Their explanation for these results was that the steric factors in packing are uniform at all compositions when the size and shape of the two components are similar and therefore the orientational cohesive energy densities will vary more or less linearly with composition to give an essentially linear curve. However, when the sizes of the two components are considerably different, the molecules are more difficult to pack together and the CM or MI transition temperatures will be

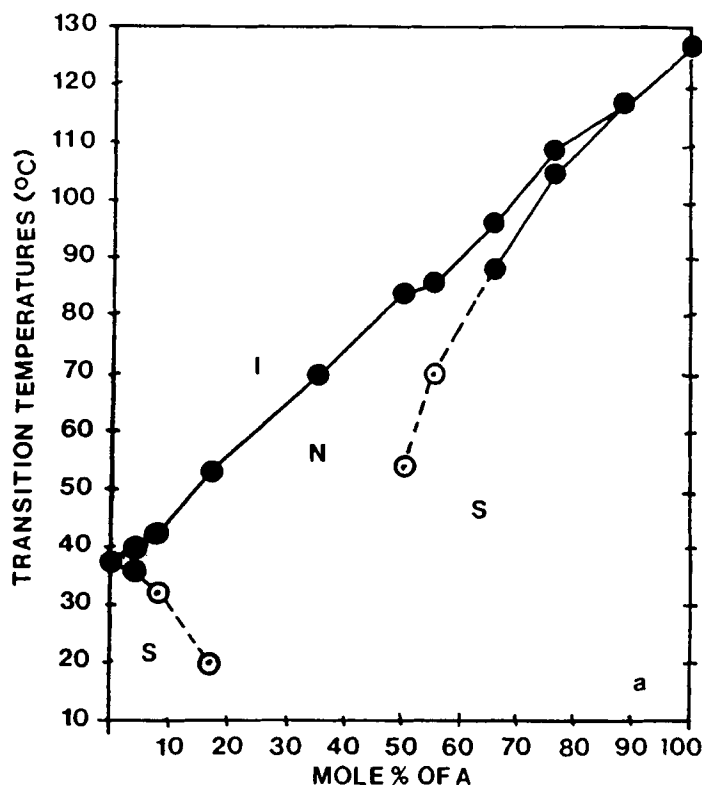
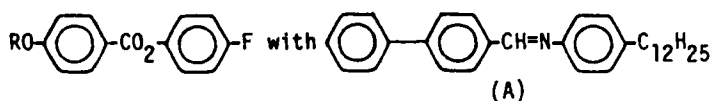


FIGURE 9 Phase diagrams for mixtures of



- a. $\text{R} = \text{C}_6\text{H}_{13}$
- b. $\text{R} = \text{C}_8\text{H}_{17}$
- c. $\text{R} = \text{C}_{10}\text{H}_{21}$

less than predicted for the ideal solution giving a non-linear plot with a minimum at the composition in which packing is the most difficult.

Our phase diagrams show these same trends but in the SN transition temperatures rather than the NI ones which form a nearly linear curve in both types of mixtures with an added INP region. When the two components have similar molecular lengths, the INP region is

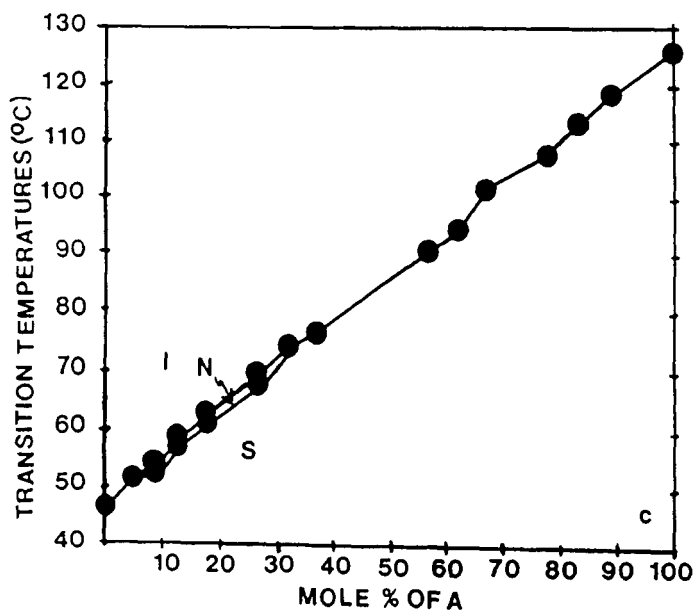
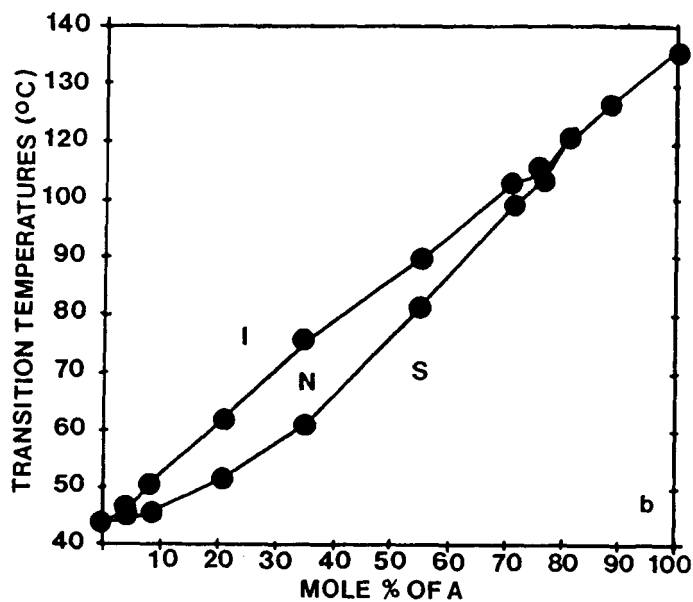


FIGURE 9 Continued

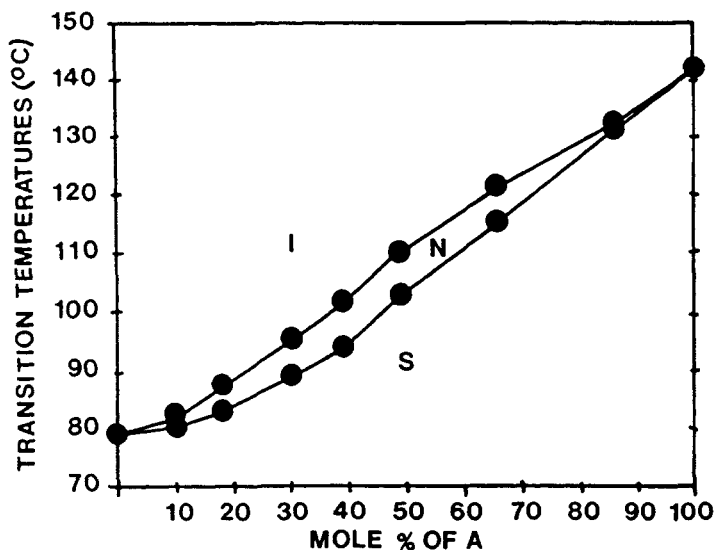
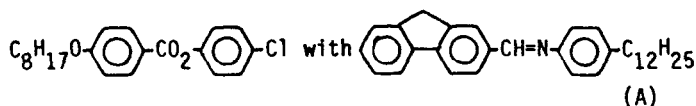


FIGURE 10 Phase diagram for a mixture of



narrow usually occurring over the entire composition range. When the molecular lengths of the two components are different, the INP occurs primarily in the dip of the non-linear SN curve having its maximum phase range in this area. It is not surprising to find that when the molecules differ in molecular length, they prefer to pack in the less ordered nematic phase rather than the more ordered smectic phases observed in the pure components. Nor is it surprising to find that this is preferred more in mixtures consisting of two different molecules than those containing two similar ones and that it is greatest at the compositions in which packing is the most difficult to achieve i.e. at the minimum in the curve.

Dave and Dewar, as well as earlier researchers, have proposed that any compound consisting of anisotropic molecules could form a mesophase if the melt could be cooled enough to observe this phase before crystallization occurred.²⁴ This provides another possible explanation for the observance of INPs in mixtures of Type I. Perhaps these two components actually have monotropic nematic phases but these are not observed because the melt crystallizes too soon. The addition of another component merely acts as an impurity lowering

TABLE XIV
Transition temperatures (°C) for the phase diagrams

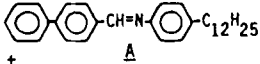
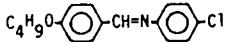
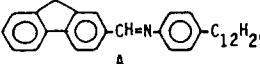
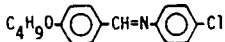
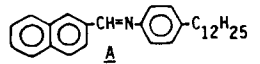
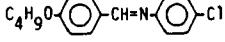
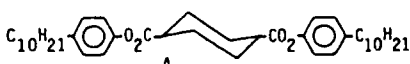
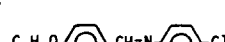
Mixture	mole % A	CN or SN	MI	L_{\max}^1
 +  (Figure 4a)	0 3.3 7.0 14.1 22.0 30.0 40.0 50.0 60.5 66.0 72.5 100.0	- - 87.6 82.7 82.0 83.9 90.0 96.8 106.0 112.6 - - - - - -	90.6 90.4 94.5 94.8 97.9 101.9 106.2 110.2 114.9 116.0 117.3 126.1	14.0
 +  (Figure 4b)	0 6.5 14.0 30.0 49.0 60.0 72.0 78.0 85.0 92.5 100.0	- - 83.5 78.6 80.7 102.5 112.9 123.4 128.3 131.1 - - - -	90.6 92.0 96.1 105.2 116.5 121.8 127.6 131.1 132.9 137.9 141.6	24.5
 +  (Figure 4c)	0 5.8 15.6 23.0 27.0 31.2 35.6 45.4 62.4 83.3 100.0	- - 76.0 68.0 60.0 46.1 49.0 57.0 - - - - (51.9) - -	90.6 79.9 76.4 71.5 67.8 65.0 61.5 ₁ 64.0 ₁ 57.6 ₂ 59.0 ₂ 52.7 62.0 141.6	21.7
 +  (Figure 4d)	0 1.4 2.5 5.0 10.0 17.0 24.0 25.5 27.5 29.0 32.0 41.0 52.0 72.0 90.0 100.0	- - 88.2 86.9 83.1 75.0 67.9 64.1 73.0 78.1 85.1 89.5 107.7 - - - - - - - -	90.6 89.8 89.9 90.7 93.6 96.7 99.4 101.7 102.3 103.6 104.6 110.8 117.4 126.1 132.9 135.2	35.3

TABLE XIV *continued*

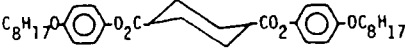
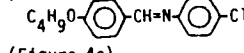
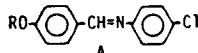
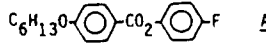
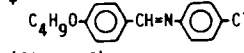
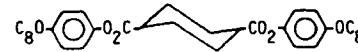
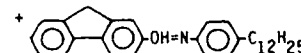
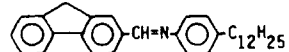
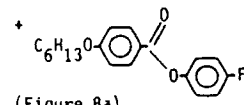
Mixture	mole % A	CN or SN	MI	L_{\max}^1
 A	0	- -	90.6	80.3
+  (Figure 4e)	2.6	87.4	93.2	
	5.4	83.5	96.0	
	11.4	76.0	107.0	
	18.1	63.9	114.8	
	25.6	55.0	122.9	
	34.1	48.3	128.6	
	36.4	86.5	132.4	
	38.7	102.7	135.6	
	43.7	113.4	138.9	
	45.7	128.9	144.5	
	60.8	146.0	152.4	
	79.2	- -	168.7	
	100.0	- -	178.0	
 A	0	- -	90.6	1.0
R = C ₈ H ₁₇ and R = C ₄ H ₉ (Figure 5)	8.5	89.3	89.6	
	17.3	88.8	89.6	
	26.4	88.9	89.9	
	51.1	- -	91.3	
	65.3	- -	94.5	
	71.5	- -	95.5	
	77.0	- -	96.4	
	88.1	- -	98.4	
	100.0	- -	100.0	
 A	0	- -	90.6	6.5
+  (Figure 6)	18.8	80.0	80.5	
	37.8	60.8	67.3	
	57.6	50.7	55.4	
	78.2	43.2	45.6	
	100.0	- -	38.3	
 A	0	- -	142.0	2.7
+  (Figure 7)	4.8	- -	142.8	
	16.4	145.0	146.8	
	34.4	151.5	154.2	
	54.1	159.8	161.2	
	75.8	- -	169.2	
	92.5	- -	175.8	
	100.0	- -	178.0	
 A	0	- -	38.3	~71
+  (Figure 8a)	3.7	35.5	39.8	
	8.0	32.8	42.8	
	19.7	~27	52.1	
	25.2	~53	61.5	
	34.4	~3	71.2	
	44.1	~15	85.0	
	54.1	~68	95.0	
	64.8	78.3	102.0	
	75.9	106.8	116.3	
	87.6	124.8	128.8	
	100.0	- -	141.6	

TABLE XIV *continued*

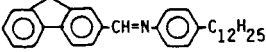
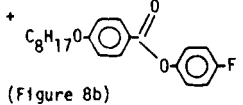
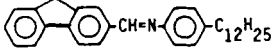
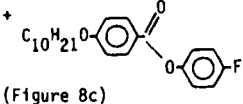
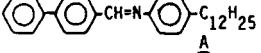
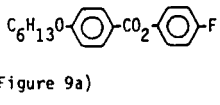
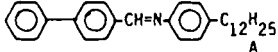
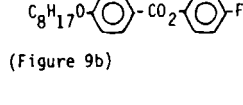
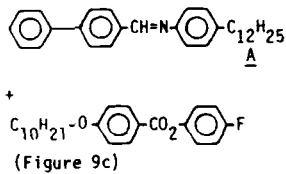
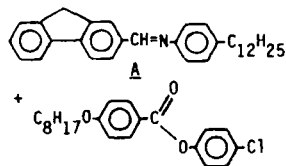
Mixture	mole % A	CN or SN	MI	L_{\max}^1
 <u>A</u>	0	- -	43.8	17.1
+  (Figure 8b)	4.0	43.8	46.7	
	8.1	44.6	50.4	
	14.7	46.6	57.5	
	16.4	47.5	59.0	
	25.2	52.4	68.8	
	30.6	60.5	76.8	
	44.1	70.0	87.1	
	59.4	88.2	100.2	
	70.2	105.1	113.2	
	78.2	114.4	120.2	
	87.6	127.7	129.1	
	100.0	- -	141.6	
 <u>A</u>	0	- -	46.3	6.6
+  (Figure 8c)	4.5	- -	51.1	
	17.6	58.6	62.4	
	26.7	65.3	71.0	
	35.6	72.5	79.1	
	46.0	84.3	90.3	
	61.2	104.5	109.5	
	77.3	118.2	119.4	
	100.0	- -	141.6	
 <u>A</u>	0	- -	38.3	14.1
+  (Figure 9a)	4.1	35.4	39.2	
	8.2	32.3	42.5	
	16.8	20.4	53.0	
	35.1	- 3	69.5	
	49.7	54.3	83.5	
	54.8	70.3	85.4	
	65.4	87.0	96.0	
	76.4	104.8	108.7	
	87.9	- -	117.0	
	100.0	- -	127.0	
 <u>A</u>	0	- -	43.8	
+  (Figure 9b)	4	44.5	46.4	
	8	45.5	50.5	
	21.0	51.7	62.0	
	35.0	61.3	75.4	
	45.0	71.2	78.3	
	55.0	81.7	89.4	
	71.0	99.9	103.0	
	76.5	102.8	104.2	
	82.0	- -	111.1	
	88.0	- -	116.9	
	100.0	- -	126.0	

TABLE XIV *continued*

Mixture	mole % A	CN or SN	MI	¹ L _{max}
 (Figure 9c)	0 9 13.0 18.0 27.0 32.0 37.0 57.0 62.0 67.0 78.0 83.0 89.0 100.0	- - 52.9 57.0 60.2 67.3 -	46.3 53.9 57.8 62.1 69.0 74.2 75.4 90.4 93.7 101.5 107.6 113.7 117.1 126.0	 1.9
 (Figure 10)	0 10.1 18.0 30.3 39.3 49.2 65.8 85.8 100.0	- - 80.4 82.7 88.7 93.6 102.8 116.2 131.4 - -	79.3 82.0 87.4 95.3 101.5 110.3 120.9 132.2 141.6	 7.9

¹ L_{\max} = maximum INP length.² The higher temperature is for $C \rightarrow I$; the lower is for the monotropic $N \rightarrow I$.³ These figures were obtained by cooling the sample rapidly to avoid crystallization. Heating temperatures for this transition could not be obtained before crystallization occurred. Therefore, these values are not accurate being lower than where the transition actually occurs. They, however, give an approximate indication as to where the true curve would occur.

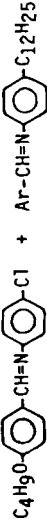
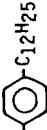
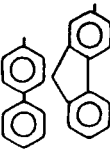

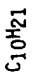
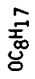
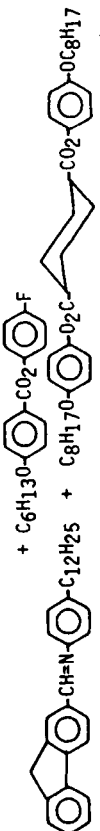


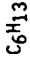
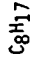
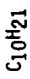
the crystallization point far enough so that the nematic phase can be observed. However, our phase diagrams show no indication that such virtual nematic phases are present. In some mixtures the nematic phases were lost at compositions containing only small amounts of the second component. In other mixtures, the SN curves obviously led to decreasing INP ranges to zero for the pure components.

EXPERIMENTAL

Materials

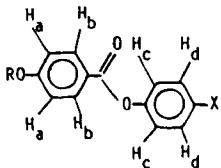
Many of the compounds used in this work had been previously prepared and reported in the literature. Esters were prepared using either the acid chloride method as described in Ref. 25 or the carbodiimide method discussed in Ref. 26. Anils were prepared by the method

TABLE XV
Differences in molecular lengths (Å) of the two components studied in phase diagrams

Mixture		Molecular Length* Difference
		12.1
		11.5
		9.8
		23.4
		17.9
		1.7
		6.4
		9.8
		7.4
		4.7
		

* Molecular lengths were measured using CPK molecular models—see data in Table XIV.

TABLE XVI

NMR chemical shift values (δ) for aromatic protons for


X	H_b	H_d	H_c	H_a
F	8.13	7.09	6.99	6.81
Cl	8.09	7.38	7.10	6.81
Br	8.09	7.50	7.05	6.90
I	8.09	7.70	6.93	6.89

described in Ref. 27. Starting materials were obtained from Commercial sources or prepared using the methods described in Refs. 28–30. The biphenyl esters were obtained from D. L. Fishel and V. Surendranath. The halo esters were purified by recrystallization from abs EtOH and their structures confirmed by IR and NMR.

NMR data for the aromatic protons in the 4-halophenyl-4'-alkoxybenzoates is presented in Table XVI. These data indicate that all these protons except those ortho to the halogen atom have essentially the same chemical shift. Those ortho to the halogen atom show an increasing chemical shift with increasing halogen size and decreasing electronegativity as one would expect. In the fluoro ester, the doublet for these protons overlap with that for those protons ortho to the ether groups. However, as the chemical shift increases, these doublets are separated. Aromatic protons ortho to the halogen in the 4-alkoxyphenyl-4'-halobenzoates also showed this effect. When the halogen was fluorine, the protons ortho to the fluorine atom were superimposed on those ortho to the two ether substituents to give an unresolved multiplet at 7.5–6.68. A set of two overlapping doublets with $J \sim 9\text{Hz}$ was observed for those protons ortho to the CO_2H . An additional splitting of these protons has also been reported in the NMR spectrum for 4-fluorobenzoic acid.³¹ When the halogen was iodide, the protons ortho to the iodide atom had the same chemical shift as those ortho to the carbonyl group giving a singlet at 7.9 and a set of doublets at 7.12 and 6.858 for the protons ortho to the ether substituents. The NMR spectrum for the 4-alkoxyphenyl-4'-nitro-

benzoates was like that for the corresponding iodo ester but with its singlet at 8.32 δ . Aromatic coupling constants were ~ 9 Hz in all cases. Aliphatic protons, except for the methylene ones adjacent to the aromatic ring or an oxygen atom, occurred as a complex multiplet at 0.5–2.0 δ in all these esters. Triplets with $J \sim 7.0$ Hz appeared for the α -methylene protons. The chemical shift of these depended on where they were attached: CH_2ArCO_2 at 2.6, $\text{CH}_2\text{OArCO}_2$ at 4.05, and OArOCH_2 at 3.98.

Microscope studies

Microscope slides and cover slips were cleaned by washing with acetone and wiping dry in one direction with a Kimwipe. Some mixtures tended to form homeotropic textures. To avoid this problem, clean slides were dipped into a 0.5% soln of polyvinyl alcohol (PVA) in H_2O and dried at 120° for 0.5–1.0 hr. This soln was prepared by dissolving 2 g of 2% Monsanto PVA in 100 ml H_2O , boiling briefly, and then cooling to RT. Storage of this soln at 5° was necessary to prevent mold growth which was used as needed to prepare the 0.5% soln by diluting 25 ml to 100 ml with H_2O . Cover slips were treated in the same manner. These were then both rubbed in the same direction parallel to the long side of the slide.

A small amount of one component was placed near the edge of the slide and an approximately equal amount of the second component placed next to the first on the side away from the edge leaving a small gap between the two. The cover slip was placed on top with the rubbed direction aligned with that of the slide. The slide was heated on a hot plate until both components melted to the isotropic liquid, ran together, and covered the entire area under the cover slip. It was then placed in a Mettler FP-2 heating stage on a Leitz-Laborlux 12POL microscope at RT. A search was quickly made by moving the slide to find the growing edge of a birefringent phase of one of the components as the sample was cooled. Once found, this edge was observed until either an INP was observed or all the melt formed a birefringent phase. Often it was necessary to move the slide as this front advanced across the melt. The INP appeared on the growing edge of a smectic phase (Figure 11), a crystalline phase or in between the growing edges of two phases (Figure 12). For most samples this could be done at RT. However, when the birefringent phase grew from the melt too rapidly, the sample was heated to a temperature high enough to slow the growing front enough so that if an INP were present, it could be observed as the sample cooled. Many times the

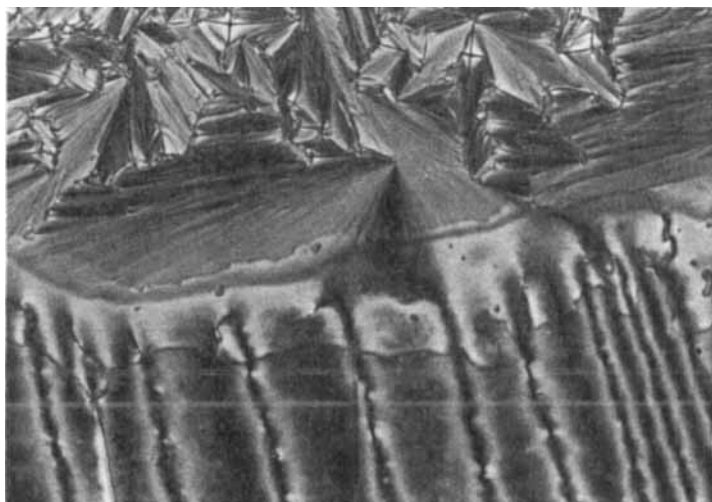
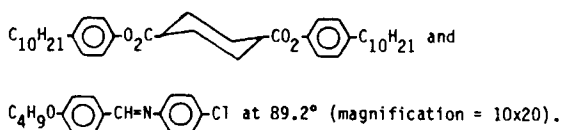


FIGURE 11 Induced nematic phase growing on the edge of the S_A phase in a mixture of

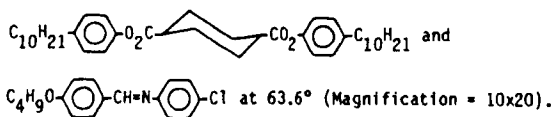


INP region was quite wide and easily detected but at other times it occurred as a narrow region or persisted only briefly and was therefore more difficult to observe. These mixtures and those which showed no INPs were studied several times and at different temperatures to be more certain whether a phase was present. This does not, however, provide absolute assurance that such a phase is not present, only that it could not be observed using these conditions. Photographs were taken using a Leitz 35 mm camera, a $20\times$ objective, and a $10\times$ eyepiece.

Samples for the phase diagrams were prepared by weighing the appropriate amounts of each component, mixing these together, melting the mixture with stirring, and then allowing it to cool to RT. This sample was placed on a slide, a cover slip added, and the sample melted and cooled until it crystallized. It was then placed in the heating stage, heated until the isotropic liquid was formed, and cooled until a birefringent phase was observed. This was reheated at $2^\circ/\text{min}$ to obtain the MI transition temperature. Another cooling to the smectic phase and reheating gave the SN transition temperature. No at-



FIGURE 12 Induced nematic phase growing between crystals and the S_A phase in a mixture of



See Color Plate IV.

tempt was made to differentiate between monotropic and enantiotropic INPs. Phase diagrams in which both components contained a smectic phase were used when possible so that SN transition temperatures could be plotted over the entire composition range simplifying the INP region. Also, only the temperatures observed for the end of a phase transition were plotted eliminating the complex mixed phase regions.

Acknowledgments

The partial financial support for this research provided by grant number DMR83-09739 from the National Science Foundation and an award from the Exxon Educational Foundation, is greatly appreciated. We are also grateful to D. L. Fishel, G. Powell, and V. Surendranath for providing the biphenyl esters; to C. Hanlon, M. Jirousek, R. Bietzel, D. Leonhardt, and F. Herlinger for synthesizing some of the materials used, to R. Bietzel and S. Laskos, Jr., for some of the phase diagrams, to the Monsanto Chemical Company for providing the PVA sample, and to the Chemistry Department for providing access to the EM360-NMR.



MOLECULAR CRYSTALS AND LIQUID CRYSTALS
COLOR PLATE III. See Ozcayir and A. Blumstein, Figure 4, see page 245.



MOLECULAR CRYSTALS AND LIQUID CRYSTALS
COLOR PLATE IV. See M.E. Neubert, K. Leung and W.A. Saupe
Figure 12, page 341.